Research Publication Repository

http://publications.wehi.edu.au/search/SearchPublications

This is the author's peer reviewed manuscript version of a work accepted for publication.

Changes introduced as a result of publishing processes such as copy-editing and formatting may not be reflected in this manuscript.

Downregulation of the GHRH/GH/IGF-1 axis in a mouse model of Börjeson-Forssman-Lehman Syndrome

Helen M. McRae[1,2], Samantha Eccles[1], Lachlan Whitehead [1,2], Warren S. Alexander[1,2], Jozef Gécz[3], Tim Thomas[1,2,*], Anne K. Voss[1,2,*]

[1]*Walter and Eliza Hall Institute of Medical Research, Melbourne, Victoria 3052, Australia*

[2]*Department of Medical Biology, The University of Melbourne, Australia*

[3]*Adelaide Medical School and the Robinson Research Institute, The University of Adelaide, Adelaide, SA, Australia*

---

* Tim Thomas and Anne K. Voss contributed equally and share senior authorship.

Correspondence should be addressed to Anne K. Voss, Email: avoss@wehi.edu.au and Tim Thomas, Email: tthomas@wehi.edu.au

Abstract

The Börjeson–Forssman–Lehmann syndrome (BFLS) is an intellectual disability and endocrine disorder caused by plant homeodomain finger 6 (*PHF6*) mutations. BFLS patients present with short stature. We report a mouse model of BFLS, in which deletion of *Phf6* causes a proportional reduction in body size compared to control mice. Growth hormone (GH) levels were reduced in the absence of PHF6. $Phf6^{-/Y}$ animals displayed a reduction in the expression of the genes encoding GH releasing hormone (GHRH) in the brain, GH in the pituitary gland and insulin-like growth factor-1 (IGF-1) in the liver. *Phf6* deletion specifically in the nervous system caused a proportional growth defect, indicating neuroendocrine contribution to the phenotype. Loss of suppressor of cytokine signaling 2 (SOCS2), a negative regulator of growth hormone signaling partially rescued body size, supporting a reversible deficiency in GH signaling. These results demonstrate that PHF6 regulates the GHRH/GH/IGF-1 axis.

Summary statement

In this paper, the authors report that loss of the plant homeodomain finger 6 (PHF6) protein) causes reversible postnatal growth retardation, mediated at least in part through neuroendocrine signaling.

Introduction

The Börjeson–Forssman–Lehmann syndrome (BFLS; OMIM 301900) is a rare intellectual disability syndrome caused by mutations in the X-linked gene *PHF6* (Borjeson et al., 1962; Lower et al., 2002). The disorder affects all known males with deleterious hemizygous *PHF6* mutations, while females heterozygous for *PHF6* mutations range from a full presentation of BFLS similar to males to apparently unaffected carriers (Berland et al., 2011; Crawford et al., 2006; Zweier et al., 2013). Neurological symptoms of BFLS include low IQ and susceptibility to seizures (Turner et al., 2004). Physical characteristics of BFLS in both males and females include deep-set eyes, large ears, tapering fingers and short toes (Turner et al., 2004). Several symptoms of BFLS including short stature, truncal obesity, gynecomastia and genital hypoplasia point to disrupted endocrine control (Turner et al., 2004).

The PHF6 protein contains two plant homeodomain zinc-fingers (Lower et al., 2002), which are domains that occur in chromatin-associated proteins implicated in transcriptional regulation (Aasland et al., 1995). Mutations of *PHF6* in BFLS occur along the length of the gene, indicating a likely loss or reduced function mechanism in the pathogenesis. PHF6 localizes to the nucleus (Lower et al., 2002) and associates with histone proteins including H3 (Soto-Feliciano et al., 2017) and histone variants including H1.2, H2B.1, H2A.Z, and H3.1 (Todd and Picketts, 2012). PHF6 has been implicated in transcriptional regulation through association with the PAF1 and NuRD complexes (Todd and Picketts, 2012). PHF6 has recently been reported to function in processes other than transcription including in non-homologous endjoining (Warmerdam et al., 2020) and as an E3 ubiquitin ligase (Oh et al., 2020). In addition to germline mutations in BFLS, somatic *PHF6* mutations occur in human hematological malignancies, including T-cell acute lymphoblastic leukemia (Van Vlierberghe et al., 2010) and acute myeloid leukemia (Van Vlierberghe et al., 2011). PHF6 has recently been proven to be a tumour suppressor (McRae et al., 2019), in addition to regulating hematopoietic stem and progenitor cell function (Hsu et al., 2019; McRae et al., 2019; Miyagi et al., 2019; Wendorff et al., 2019).

A recent report characterized the neurological features of a mouse model of BFLS with a patient-specific mutation involving replacement of cysteine 99 in the first PHF6 PHD finger with phenylalanine (PHF6[C99F]) (Cheng et al., 2018). These mice

displayed reduced levels of PHF6 protein, evidence of deficits in contextual and social recognition memory and increased seizure susceptibility in response to epilepsy-inducing drugs (Cheng et al., 2018). Mice with the PHF6^{C99F} mutation were reported to weigh less and have reduced body length (Cheng et al., 2018), recapitulating the short stature observed in BFLS. The mechanisms underpinning this growth defect have not been investigated.

The hypothalamic-pituitary axis controls endocrine function in mammals. Transcription and secretion of the anterior pituitary hormones, growth hormone (GH), thyroid stimulating hormone (TSH), adrenocorticotrophic releasing hormone (ACTH) and the gonadotropins luteinizing hormone (LH) and follicle stimulating (FSH) are stimulated by their respective hypothalamic releasing hormones, including growth hormone releasing hormone (GHRH), thyrotrophin releasing hormone (TRH), corticotrophin releasing hormone (CRH) and gonadotropin releasing hormone (GnRH) (Chrousos et al., 2009; Ikegami and Yoshimura, 2017; Ranke and Wit, 2018; Stamatiades and Kaiser, 2018; Thackray et al., 2010), while prolactin (PRL) secretion is primarily controlled via negative regulation by dopamine (Bernard et al., 2019). The anterior pituitary hormones (GH, TSH, LH, FSH, ACTH and PRL) are secreted into the bloodstream and in turn regulate production of downstream hormones at peripheral sites. Pituitary hormones exert pleiotropic effects, including the control of growth in the case of the GH and thyroid axes (Ikegami and Yoshimura, 2017; Ranke and Wit, 2018).

Endocrine testing of BFLS patients has revealed alterations in pituitary hormone levels in some patients (see Table S1, adapted from a summary by Zhang and colleagues (Zhang et al., 2019)). Specifically, GH was found to be lower than average in 3 of 4 males (Birrell et al., 2003; Dereymaeker et al., 1986; Robinson et al., 1983) and 3 of 4 females assayed (Petridou et al., 1997; Robinson et al., 1983; Zhang et al., 2019). TSH was decreased in 2 of 4 assessed males (Birrell et al., 2003; Dereymaeker et al., 1986; Robinson et al., 1983; Turner et al., 1989; Weber et al., 1978) and increased in one of 5 assessed females (Birrell et al., 2003; Carter et al., 2009; Crawford et al., 2006; Matsuo et al., 1984; Petridou et al., 1997; Robinson et al., 1983; Zhang et al., 2019). Since both the GH and thyroid axis control growth (Wit et

al., 2016), it is possible the reduced function of one or both of these pathways is responsible for the observed short stature in BFLS.

PRL levels were reported to be unchanged in one male tested (Robinson et al., 1983), and 3 females tested (Petridou et al., 1997; Robinson et al., 1983), while ACTH deficiency was mentioned in a case report of two brothers (Birrell et al., 2003). Testosterone levels were commonly affected, with 11 of 14 males showing a decrease (Ardinger et al., 1984; Baumstark et al., 2003; Carter et al., 2009; de Winter et al., 2009; Robinson et al., 1983; Turner et al., 1989; Weber et al., 1978). Levels of the gonadotropins LH and FSH were up in some cases but down in others (Table S1), leading to the hypothesis that BFLS may involve both central and peripheral defects of the gonadotropin axis (Robinson et al., 1983).

It is important to note that these endocrine tests have been performed in various laboratories over a span of more than 40 years. Consequently, it is unclear whether the discrepancy in results represents true variation between patients (perhaps due to different genetic variants in the *PHF6* gene, polymorphisms in the genetic background and/or environmental factors), variable testing procedures, or other factors such as the age at which patients were tested.

While the endocrine test results are variable among BFLS patients, the symptoms of BFLS including frequent short stature (with a normal birth weight), small genitalia and gynecomastia (Gecz et al., 2006), along with altered pituitary hormone levels identified in a number of BFLS patients led us to hypothesize that loss of PHF6 may disrupt hypothalamic-pituitary axis function. Therefore, we sought to characterize the role of PHF6 in regulation of this axis. Here, we report the phenotype of a novel mouse model of BFLS and identify PHF6 as a key regulator of the GHRH/GH/IGF-1 axis, which controls growth, at least in part, through regulation within the nervous system.

Results

Mice lacking PHF6 survive on the FVB/BALB/C background and display a postnatal growth defect

To study the role of PHF6 in the endocrine system, we used a murine *Phf6* allele with *loxP* sites flanking exon 4 and 5 (McRae et al., 2019), which results in undetectable *Phf6* mRNA upon cre-mediated recombination (Fig. S1A). As previously reported,

males with germline deletion of *Phf6* on a C57BL/6 background died shortly after birth, while heterozygous females survive to adulthood (McRae et al., 2019). Female mice with germline mutation in one copy of *Phf6* had a significantly reduced body weight compared to control mice (p < 0.001, Fig. 1A). A significant difference was detected by 3 weeks of age using Bonferroni's post-hoc test for multiple comparisons (7.47 ± 0.33 g vs. 9.00 ± 0.25 g for *Phf6*$^{+/-}$ and *Phf6*$^{+/+}$ mice, respectively, p = 0.01, Fig. 1A). Male *Phf6*$^{-/Y}$ mice isolated just before birth at E18.5 had an equal body weight compared to controls (1.13 ± 0.04 g vs. 1.13 ± 0.05 g, p = 0.96; Fig. S1B), indicating the effect of PHF6 on growth and survival occurs postnatally.

The survival of human BFLS patients with mutations expected to result in complete loss of PHF6 suggest that hemizygous *PHF6* loss of function mutations should be compatible with postnatal life. We hypothesised that the genetic background may be an important determinant of survival. In order to model an outbred genetic background that may more closely represent the effect of loss of function mutations in humans, we bred the *Phf6*$^-$ allele onto a mixed FVB/BALB/c background. In contrast to the C57BL/6 background, *Phf6*$^{-/Y}$ males survived postnatally on the mixed FVB/BALB/c background, although they were slightly underrepresented by weaning with 17.7% vs. the expected 25% (p = 0.0498; Table S5), for reasons yet to be determined. Once weekly weighing showed that adult *Phf6*$^{-/Y}$ mice have a reduction in body weight compared to wild-type mice (p < 0.001), with a significant difference detected by 2 weeks of age with Bonferroni's post-hoc test for multiple comparisons (5.13 ± 0.45 g, vs. 8.27 ± 0.39 g, p < 0.001; Fig. 1B. The largest difference in body weight was at 3 weeks of age where *Phf6* deleted mice were approximately 50% smaller than controls (5.40 + 0.66 vs. 10.72 + 0.47, p < 0.001; Fig. 1B). Body length (79.75 ± 2.02 mm vs. 96.00 ± 1.08 mm) and femur length (9.75 ± 0.32 mm vs. 11.75 ± 0.14 mm) was significantly reduced in *Phf6*$^{-/Y}$ mice compared to controls (p = 0.0004 and 0.001, respectively; Fig. 1C-E), indicating the reduced body weight is a result of reduced overall growth rather than reduced adipose tissue. Indeed, relative to body weight, *Phf6*$^{-/Y}$ mice had an increase in the inguinal subcutaneous and dorsal lumbar white fat compared to controls (0.019 ± 0.002 g vs. 0.011 ± 0.001 g, respectively, p = 0.02), but no change in the interscapular brown adipose tissue (Fig. 1F). In absolute terms, the lean body volume, but not the adipose tissue volume, was significantly reduced in the *Phf6*$^{-/Y}$ mice compared to controls (Fig. 1G). Males of the *Phf6*$^{-/Y}$ genotype were fertile. Intercrosses between *Phf6*$^{-/Y}$

and *Phf6⁻/⁺* demonstrated that FVB/BALB/c females with homozygous mutation in *Phf6* could survive and, as was demonstrated for *Phf6⁻/⁺* heterozygous females, they were smaller than control females (10.41 ± 0.80 g, 8.32 ± 0.33 g and 7.00 ± 0.01 g for *Phf6⁺/⁺*, *Phf6⁻/⁺*, *Phf6⁻/⁻* genotypes respectively at 3 weeks of age; p = 0.01 for *Phf6⁻/⁻* vs. *Phf6⁺/⁺*, p = 0.02 for *Phf6⁻/⁺* vs. *Phf6⁺/⁺*; Fig. S1C).

Phf6 deletion results in reduced GH secretion and reduced pituitary gland GH levels

To test whether the loss of PHF6 altered circulating levels of pituitary hormones, we assayed the concentrations of ACTH, GH, FSH, LH, PRL and TSH using a multiplex assay in male mice on the FVB/BALB/c background. Because of the pulsatile nature of pituitary hormone secretion (Steyn et al., 2011; Steyn et al., 2013), we assayed blood isolated every 10 minutes over 6 hours (Fig. 2A, Fig. S2).

Given the smaller size of the $Phf6^{-/Y}$ animals, we hypothesised that there would be lower levels of GH. As expected, $Phf6^{-/Y}$ mice displayed a 1.8-fold reduction in the mean concentration and total secreted GH (area under the curve) compared to control mice (Fig. 2A, Table 1). Deconvolution analysis using the *AutoDecon* algorithm (Johnson et al., 2008; Johnson et al., 2009) indicated that the basal secretion rate of GH and the number of peaks were unaffected by PHF6, but there was a 6.4-fold decrease in the maximum peak mass and a 6.8-fold decrease in the average peak mass in $Phf6^{-/Y}$ animals compared to $Phf6^{+/Y}$ littermates (Table 1).

To test whether the reduction in secreted GH levels corresponded to a reduction in pituitary GH levels, we performed western blots for GH using pituitary lysates and observed a reduction in GH protein, relative to the actin loading control, in $Phf6^{-/Y}$ pituitaries versus $Phf6^{+/Y}$ controls (Fig. 2B,C). These results indicate that pituitary GH and secreted GH levels are decreased in mice lacking PHF6.

Effect of PHF6 on other hypothalamic-pituitary axis pathways

In contrast to the effect of PHF6 on GH secretion, there was no effect of PHF6 loss on the concentration or secretion parameters of the other pituitary-derived hormones assessed; ACTH, FSH, LH, PRL and TSH (Fig. S2, Tables S6-S10). Despite no change in the circulating levels of ACTH, FSH, LH, PRL and TSH between $Phf6^{-/Y}$ and control mice, we identified changes in the mRNA levels in hypothalamic pituitary axis genes of some of these pathways through assessing a panel of candidate genes by

RT-qPCR. In male FVB/BALB/c $Phf6^{-/Y}$ mice, we found reduced mRNA levels of the prolactin gene, *Prl* in the pituitary gland (Fig. S3A). Levels in the pituitary gland of the pro-opiomelanocortin gene, *Pomc,* which encodes the ACTH precursor, were significantly reduced in $Phf6^{-/Y}$ versus control adult mice, whereas corticotrophin-releasing hormone (*Crh*) mRNA levels, encoding the *Pomc* stimulating factor, were unchanged in the brain (Fig. S3B-C). Pituitary transcript levels of the gene encoding the common alpha subunit (*Cga*) for TSH, FSH, and LH, the thyrotropin releasing hormone beta subunit (*Tshb*), and the gonadotropin beta subunits (*Fshb* and *Lhb),* were not affected by *Phf6* status (Fig. S3D-G). *Trh* mRNA levels were unaffected in the adult brain (Fig. S3H), however, gonadotropin releasing hormone (*Gnrh1*) transcripts were slightly reduced in the brain of adult $Phf6^{-/Y}$ versus control mice (Fig. S3I). These results indicate some evidence of a minor effect of PHF6 on the central hypothalamic-pituitary-gonadal axis in the form of an effect on brain *Gnrh1* mRNA levels, in addition to reduced pituitary gland transcript levels of *Prl* and *Pomc* caused by loss of PHF6. However, these changes at the mRNA level did not manifest as corresponding changes to the circulating levels of gonadotropins, PRL or ACTH proteins in FVB/BALB/c mice.

Deletion of Phf6 results in reduced mRNA levels of GHRH/GH/IGF-1 axis genes

Assessment of transcript levels of endocrine genes in the GH pathway in mice on the FVB/BALB/c background demonstrated a significant reduction in mRNA levels of the growth hormone releasing hormone gene (*Ghrh*) in the brain of adult mice lacking PHF6 (Fig. 3A). On the other hand, loss of PHF6 had no effect on the expression of somatostatin (*Sst*), a negative regulator of GH release and secretion (Fig. 3B). In concordance with the reduced GH pituitary protein levels, transcripts of the growth hormone gene, *Gh,* in the pituitary gland were also significantly reduced both at PN14 and in adults (Fig. 3C). Transcript levels of the downstream effector gene of GH, *Igf1,* were reduced in the liver at PN14 and in older mice in the absence of PHF6 ($Phf6^{-/Y}$) compared to controls (Fig. 3D). The absence of PHF6 ($Phf6^{-/Y}$) also resulted in a reduction in plasma IGF-1 protein levels (Fig. 3E). These results indicated that downregulation of the GHRH/GH/IGF-1 axis is likely to be responsible for the observed growth defect resulting from loss of PHF6.

Nervous system specific deletion of Phf6 results in a postnatal growth defect

The effect of PHF6 on transcription of GHRH/GH/IGF-1 axis genes in the brain, pituitary gland and liver suggests that PHF6 could be playing a role in multiple tissues and at multiple levels of the GHRH/GH/IGF-1 axis. To assess whether a neuroendocrine role of PHF6 was contributing to the growth defect, we employed the *Nestin-cre* transgene, which is expressed in the nervous system, including the hypothalamus, but not in the pituitary gland or the liver (Tronche et al., 1999). By crossing *Phf6* (*Phf6*$^{\text{lox}}$) mice with mice expressing the *Nestin-cre* transgene (*Nes-cre*$^{\text{Tg/+}}$), we deleted *Phf6* specifically in the nervous system on the C57BL/6 background (Fig. S4A-B). Males with nervous system deletion of *Phf6* (*Phf6*$^{\text{lox/Y}}$;*Nes-cre*$^{\text{Tg/+}}$) survived postnatally on the C57BL/6 background, indicating the perinatal death observed in C57BL/6 *Phf6*$^{-/\text{Y}}$ mice was not due to nervous system specific effects. Since the *Nestin-cre* transgene alone causes a mild postnatal growth defect (Declercq et al., 2015; Galichet et al., 2010), evident by 4 weeks of age (Fig. S4C), we compared *Phf6*$^{\text{lox/Y}}$;*Nes-cre*$^{\text{Tg/+}}$ mice to *Nes-cre*$^{\text{Tg/+}}$ controls to measure the effect of *Phf6*-deletion specifically. *Phf6*$^{\text{lox/Y}}$;*Nes-cre*$^{\text{Tg/+}}$ mice displayed a reduction in body weight compared to *Phf6*$^{+/\text{Y}}$;*Nes-cre*$^{\text{Tg/+}}$, with a statistically significant difference in multiple comparisons evident by postnatal week 3 (9.06 ± 0.52 vs. 5.13 ± 0.30 respectively) corresponding to a 43% reduction in body weight ($p < 0.001$; Fig. 4A). This effect was proportional, affecting overall body size (Fig. S4D). The effects of nervous system-specific deletion of *Phf6* were accompanied by a reduction in *Igf1* mRNA in the *Phf6*$^{\text{lox/Y}}$;*Nes-cre*$^{\text{Tg/+}}$ liver compared to controls (Fig. 4B). The effects of nervous system-specific deletion of *Phf6* on overall body growth and peripheral organs demonstrate that control of body growth by PHF6 is at least in part mediated by neuroendocrine signaling.

Anterior pituitary gland cells produce a reduced amount of growth hormone

A reduction in anterior pituitary hormone protein in the pituitary gland in the absence of PHF6 (see GH in Fig. 2B,C) could result from a reduction in the number of hormone producing cells as a result of a defect in pituitary development or from a reduction in the amount of hormone produced per cell. To distinguish these two possibilities, we assessed the histology of the pituitary and GH, PRL, ACTH, TSH and FSH levels per cell by immunofluorescence in sections of *Phf6*$^{+/\text{Y}}$ and *Phf6*$^{-/\text{Y}}$ pituitary glands (Fig. 5; Fig. S5). The pituitary gland displayed a normal histological

structure (Fig. 5A), but was smaller in $Phf6^{-/Y}$ mice compared to controls (not shown). Likewise, the volume of the anterior lobe specifically was smaller in $Phf6^{-/Y}$ mice than in control mice (Fig. 5B). However, the decrease in volume was proportional to the decrease in total body volume (Fig. 5C). The absence of PHF6 caused a reduction in GH immunofluorescence signal per cell and per animal (Fig. 5D,E,F), but not in the GH+ area or the total GH+ cell number. Similarly, the PRL signal was reduced per cell $Phf6^{-/Y}$ mice compared to controls, but not the PRL+ area (Fig. S5A). Only ACTH, in addition to being reduced per cell, appeared to be present in a smaller area of the tissue in $Phf6^{-/Y}$ mice compared to controls (Fig. S5B). No significant differences were observed in TSH or FSH staining (Fig. S5C,D). These results suggest that PHF6 is required either directly or indirectly for the production of normal levels of GH, PRL and ACTH per cell and possibly also for the development or survival of normal numbers of ACTH producing cells.

The growth defect caused by loss of PHF6 is reversible by abolishing the negative regulation of GH signaling by the suppressor of cytokine signaling 2

Suppressor of cytokine signaling (SOCS) proteins provide important negative feedback mechanisms for many signaling pathways. SOCS proteins act by binding to and blocking activation of phosphorylation sites and by serving as E3 ubiquitin ligase adapter proteins, committing signal cascade proteins to proteasomal degradation (Linossi et al., 2013; Rico-Bautista et al., 2006). SOCS2 is an important negative regulator of growth hormone receptor (GHR) signaling and as such, $Socs2^{-/-}$ mice display gigantism and elevated $Igf1$ levels in several tissues (Favre et al., 1999; Greenhalgh et al., 2005; Metcalf et al., 2000).

To investigate whether upregulation of the GHRH/GH/IGF-1 pathway could rescue the growth defects of $Phf6^{-/Y}$ mice, we generated $Phf6;Socs2$ double mutant mice and determined the effects of loss of SOCS2 on the $Phf6^{-/Y}$ growth defect. We bred the $Socs2^{-/-}$ mice for 3 generations onto the mixed FVB/BALB/c background. Strikingly, deletion of $Socs2$ partially rescued the growth defect resulting from loss of PHF6, with a significant increase detected by multiple comparisons between $Phf6^{-/Y};Socs2^{+/+}$ and $Phf6^{-/Y};Socs2^{-/-}$ mice from five weeks of age onwards (11.71 ± 1.65 g vs. 16.98 ± 1.30 g at 5 weeks, p = 0.04; Fig. 6A, Table S11). After 8 weeks, there was no statistically significant difference between the double mutant $Phf6^{-/Y};Socs2^{-/-}$ and wild type $Phf6^{+/Y};Socs2^{+/+}$ mice, demonstrating a distinct rescue (27.78 ± 1.13 g vs.

24.42 ± 0.73 g respectively at 8 weeks, p = 0.29; Fig. 6A, Table S11). Consistent with an effect on skeletal growth, deletion of *Socs2* increased the femur length of *Phf6*^{−/Y} mice (Fig. 6B-C). These results indicate that the growth defects caused by loss of PHF6 can be reversed by elevated GH signaling.

Discussion

An analysis of 19 BFLS patients showed that 47% of BFLS males have a height that is more than two standard deviations below the population average (Turner et al., 2004). Body size is controlled by both environmental and genetic factors (Grasgruber et al., 2014; Grunauer and Jorge, 2018; Lango Allen et al., 2010; Perkins et al., 2016). Genetic variants that impact body size typically have either a described role in cell proliferation (Bicknell et al., 2011a; Bicknell et al., 2011b; Griffith et al., 2008; Guernsey et al., 2011; Klingseisen and Jackson, 2011; Rauch et al., 2008) or endocrine function (Abuzzahab et al., 2003; Pfaffle and Klammt, 2011; Phillips et al., 2001; Pugliese-Pires et al., 2011; Wajnrajch et al., 1996; Wit et al., 2016). In this paper, we have shown that PHF6 is an important regulator of postnatal growth, and that deletion of germline *Phf6* in mice, models the short stature of BFLS patients. The proportional growth defect resulting from *Phf6* deletion specifically within the nervous system indicates that PHF6 controls growth at least in part through neuroendocrine regulation.

Role of PHF6 in regulating the GHRH/GH/IGF-1 axis

We have demonstrated that the GHRH/GH/IGF-1 axis is a key pathway downregulated by loss of PHF6. We identified reduced transcription of *Ghrh* in the brain*, Gh* in the pituitary gland*,* and *Igf1* in the liver. Since GHRH regulates the transcription and secretion of *Gh* (Barinaga et al., 1983)*,* which in turn regulates transcription of *Igf1* (Lupu et al., 2001), it is possible that the effects on *Gh* and *Igf1* mRNA could be an indirect downstream result of the reduction in *Ghrh.* Indeed, if the primary effect was GH or IGF-1 reduction, increased *Ghrh* expression would be expected due to alleviation of the negative feedback loop (Phelps et al., 1993). Furthermore, the effect of *Phf6* deletion appears to be similar to the *Ghrh* (Alba and Salvatori, 2004), *Ghrhr* (Eicher and Beamer, 1976), and *Ghr* (Lupu et al., 2001; Meyer et al., 2004; Zhou et al., 1997) mutant mice which display postnatal growth

defects. In contrast, *Igf1* mutant mice are already approximately 60% smaller than controls at birth (Baker et al., 1993; Liu et al., 1993; Powell-Braxton et al., 1993). These observations, combined with the finding that nervous system-specific deletion of *Phf6* is sufficient to cause a growth defect, are consistent with a primary effect of PHF6 on regulating *Ghrh*. Notwithstanding, it is possible that PHF6 may also play an additional role in regulating *Gh* expression in the pituitary gland and *Igf1* in the liver, since *Phf6* is also expressed in these tissues (Voss et al., 2007). Further work is required to establish the exact molecular mechanisms by which PHF6 regulates endocrine pathways. Interestingly, PHF6 has been co-immunoprecipitated with PHIP (BRWD2), a reader of methylated H3K4 (Morgan et al., 2017), which has been shown to potentiate the effects of IGF-1 signaling (Podcheko et al., 2007). *PHIP* mutations have been described in humans with developmental delay and intellectual disability (Jansen et al., 2018; Webster et al., 2016) while mice lacking the full length PHIP protein display a postnatal growth defect (Li et al., 2010). Therefore, investigation into whether PHF6 interacts with PHIP to control the GH/IGF-1 axis may offer insights towards our understanding of the molecular details of how PHF6 controls the GH/IGF-1 pathway.

Rescue of growth defect caused by loss of PHF6

The rescue of the growth defect in *Phf6*$^{-/Y}$ mice by additional deletion of *Socs2* demonstrates that loss of negative regulation of GH signaling is able to override the effects caused by loss of PHF6, supporting the hypothesis that PHF6 regulates the GHRH/GH/IGF-1 axis. We conclude that the level of GH in the absence of PHF6 must be sufficient to enable the lack of negative regulation by SOCS2 to rescue the growth defect (in contrast to the *Ghrhr* knockout *"little"* mouse, in which the almost complete absence of GH renders mice unresponsive to deletion of *Socs2*) (Greenhalgh et al., 2005). These results provide a proof of principle that the growth defect caused by *Phf6* mutation can potentially be rescued with GH treatment. However, it will be important for clinicians to consider whether the potential benefits of GH treatment for human BFLS patients will outweigh the risks (Allen, 2006; Radcliffe et al., 2004). A 9-year-old female BFLS patient recently treated with daily growth hormone injections developed oedema after 3 weeks of treatment (Zhang et al., 2019). Furthermore, treatment with growth enhancers must be carefully considered in the context of *PHF6* mutations being associated with leukemia (Van Vlierberghe et al., 2010). Two BFLS

patients have developed hematopoietic malignancy (Carter et al., 2009; Chao et al., 2010). PHF6 regulates hematopoietic stem and progenitor cells (McRae et al., 2019; Wendorff et al., 2019), and notably, mice with germline or blood-specific mutation of *Phf6* have an accelerated onset of hematopoietic malignancy compared to controls (McRae et al., 2019), establishing PHF6 as a bona fide tumor suppressor. This indicates that further BFLS patients may be susceptible to leukemia. While long-term studies have found no overall increased risk of leukemia with GH treatment in patients with no known risk factors (Allen et al., 1997; Stochholm and Kiess, 2018), GH-treated patients with predisposing factors may be at higher risk (Nishi et al., 1999; Watanabe et al., 1993; Watanabe et al., 1988), thus endocrine therapies for BFLS patients should be approached with consideration of these additional factors.

Role of PHF6 in regulating other hypothalamic-pituitary axis pathways

Despite having not observed a significant effect on PRL or ACTH secretion, we found that *Prl* and *Pomc* transcripts were downregulated in the pituitary gland and that PRL and ACTH levels per cell were reduced. Similarly, while we did not observe an effect on FSH or LH secretion, nor mRNA levels, the levels of *Gnrh1* mRNA in the hypothalamus were reduced. The symptoms of BFLS that these pathways may be related to (such as genital hypoplasia and gynecomastia) do not appear to manifest in mice. Any effect of PHF6 on these pathways at the transcriptional level appears to be compensated for, resulting in normal secretion levels in mice. Whether these pathways are important in the pathogenesis of human BFLS will be an important avenue for further research.

Mutation type and genetic background are important mediators of the effects of Phf6 mutation

At least three infants with BFLS have been treated for failure to thrive and a further two developed hypoglycaemia in the neonatal stage (Turner et al., 2004). Two deaths have been reported in childhood BFLS; one male at 2 years with severely retarded growth and another male at 4 years who presented with a respiratory illness (Birrell et al., 2003; Turner et al., 2004). No direct correlation between the specific *PHF6* mutation and the severity of presentation has been defined for BFLS in humans (Turner et al., 2004). The survival of PHF6[C99F] hypomorphic mutant mice on the C57BL/6 background (Cheng et al., 2018) in contrast to the perinatal death of

C57BL/6 mice with loss of function *Phf6* mutation demonstrated here, and reported in another loss of function *Phf6* model (Cheng et al., 2018), suggests that there is indeed an effect of mutation type on phenotypic presentation. The survival of FVB/BALB/c *Phf6*$^{-/Y}$ males shown here in contrast to the perinatal death of C57BL/6 *Phf6*$^{-/Y}$ males implicates the genetic background as an important additional mediator of the severity of phenotype presentation. Therefore, the specific *PHF6* mutation inherited in addition to the overall genetic makeup of the individual is likely to influence the presentation of symptoms in BFLS. Environmental factors are also likely to mediate the impact of PHF6 mutations, as it has recently been shown that loss of PHF6 specifically in AgRP neurons has no effect on body weight in mice on an *ad libitum* diet, however mice lacking PHF6 in AgRP neurons on an alternate fasting/feeding diet have reduced feeding and reduced body weight (Gan et al., 2020).

Overall, we have shown that PHF6 positively controls postnatal growth, at least in part through neuroendocrine signaling. We have demonstrated that PHF6 is an important regulator of the GHRH/GH/IGF-1 axis; specifically in levels of pituitary GH and secreted GH and of *Ghrh, Gh* and *Igf1* transcript levels. This study provides a better understanding of the etiology of BFLS and further insight into the genetic control of the endocrine system.

Materials and methods

Animals

The *Phf6*^{lox} targeted deletion allele was previously described (McRae et al., 2019) and was used in combination with cre-deleter mice (Schwenk et al., 1995) for germline deletion. The *Nestin-cre* transgene (Tronche et al., 1999) was crossed to *Phf6* mice with the *Phf6*^{lox} targeted deletion allele mice maintained on a C57BL/6 background. As hemizygous *Phf6* deletion is perinatal lethal on a C57BL/6 background (McRae et al., 2019), mice were crossed to F1 hybrid FVB/BALB/c mice as we have done previously (Thomas et al., 2006), and kept on a mixed genetic background with 50% FVB and 50% BALB/c contribution by crossing to F1 hybrid FVB/BALB/c mice in every generation. C57BL/6 mice with the *Socs2* null allele (Metcalf et al., 2000) were crossed for at least 3 generations to F1 FVB/BALB/c mice prior to experimental use.

Genotyping was performed using primers as described in Table S2. All experimental procedures complied with the animal ethics regulations of the NHMRC of Australia and with approval of the WEHI Animal Ethics Committee.

Inclusion, exclusion and randomisation

No animals were excluded. We possible, automated assessment was used to avoid biases, e.g. multiplex hormone assays, automated image analysis (micro-CT, immunofluorescence), densitometry of western blots and RT-qPCR.

Repeat blood sampling

The sampling procedure, adapted from Steyn and colleagues (Steyn et al., 2011) used a modified version of the tail-clip blood collection procedure (Abatan et al., 2008). A scalpel blade was used to create a small (1-2 mm) cut at the tail tip, followed by the collection of 4 µL of whole blood using a P20 pipette from the tail tip every 10 minutes over 6 hours. 4 µL of blood was added to 22 µL of 3.38 mM EDTA in PBS, immediately spun for 5 minutes at $2000 \times g$ to isolate the supernatant which was snap frozen on dry ice before being stored at –80°C until analysis. The experiment was repeated a total of three times, with each experiment involving one $Phf6^{-/Y}$ animal and a $Phf6^{+/Y}$ littermate control.

Micro-CT assessment of body composition

Samples were imaged using a Bruker Skyscan 1276 Micro-CT system. Imaging parameters were set to balance contrast with acquisition time and resolution, and images were acquired with 41 μm^3 voxels. The x-ray projection images were reconstructed into 3D volumes using Bruker's NRecon software, before being analysed in FIJI using a custom written macro. Briefly, the images were run through a series of intensity and morphology filters, before being thresholded to remove signal from bone, skin, and other organs. Total volumes of the animal, as well as the adipose tissue were recorded.

Hormone assay and data analysis

The multiplex pituitary hormone assay (MPTMAG-49K, Millipore) with beads to ACTH, FSH, GH, Prolactin, TSH and LH was performed as per the manufacturer's instructions, in technical duplicates for each time point. The plates were read on the

Luminex 200 3.1 xPONENT System. Standard curves and concentration values were obtained using the Milliplex Analyst 5.1 Software. Technical duplicates were averaged prior to deconvolution analysis and only excluded in the rare cases where no value for that analyte was returned from the multiplex assay. Precision values for the *AutoDecon* program were calculated as described (Johnson et al., 2008) using the minimal detectable concentration and the coefficient of variation values provided by the multiplex kit manufacturer. The *AutoDecon* algorithm (Johnson et al., 2008; Johnson et al., 2009) was run independently for each animal and hormone with the peak triage p-value set to 0.15 and software-estimated values for the secretion standard deviation and the half-life.

Serum IGF-1 levels were measured using a Quantikine ELISA kit for IGF-1 (RnD Systems, Cat #MG100) according to the manufacturer's instructions.

Western blot

Pituitary gland lysates were derived from micro dissected pituitary glands using KALB lysis buffer (1% Triton X, 1mM EDTA, 150mM NaCl, 50mM Tris HCl pH 7.4, 0.02% NaN3) and proteinase inhibitors (Roche). Denatured lysates were separated by electrophoresis on a 4-12% NuPAGE Bis-Tris gel, and transferred onto a PVDF membrane (Osmonics). Membranes were blocked with 5% skim-milk/PBST, probed with anti-GH IgY antibody (XW-7687, Pro-Sci) followed by anti-IgY-HRP secondary (sc-2428, Santa Cruz), or anti-actin-HRP (sc-1616, Santa Cruz). Blots were developed on film using chemiluminescence and scanned for densitometry.

Immunofluorescence

The pituitary was dissected and positioned horizontally in a cryomold (Tissue-Tek, Y557) pre-filled with O.C.T. mounting medium (Tissue-Tek, IA018) then immediately snap-frozen on dry ice before storage at -80°C. Specimens were sectioned in 5 µm sections using a Microm HM525 Cryostat and placed on Superfrost positively charged slides, air-dried briefly, then placed on dry ice and stored at -80°C. For immunofluorescence staining, frozen sections were fixed in 4% (w/v) PFA (Sigma, 158127-500G) in phosphate buffered saline (PBS) for 30 mins, followed by permeabilisation in 0.2% (v/v) Triton-X-100 (Sigma, T8787), then blocking PBSG (0.25% (w/v) gelatine (Sigma, G-1890) in PBS) for 15 mins each. Sections were incubated with primary antibody diluted in PBSG for 1 hour in a wet chamber at room

temperature. Antibodies used were raised against GH (XW-7687, Pro-Sci; 1:100), ACTH (orb10034, Biorbyt; 1:25), prolactin (orb4237, Biorbyt 1:20), FSH (MA5-14711, Thermo Fisher; 1:50) and TSH (LS-C50523, Lifespan Biosciences: 1:100). Thereafter, sections were washed 3 times in PBS for 5 min each, then incubated with secondary antibody for 1 hour. Sections were rinsed in PBS and counterstained with 0.1 µg/mL of DAPI (Sigma, 10236276001) for 5 mins at room temperature, rinsed in PBS then mounted with Dako fluorescence mounting medium (Dako, S3032). Slides were stored in the dark at 4°C and imaged 1-3 days after staining. Images were acquired on a compound fluorescence microscope (Axioplan 2, Zeiss) using a digital camera (AxioCam HR, Zeiss). Mean fluorescence intensity per cell was determined in areas of 112,230 μm^2 to 142,800 μm^2 per animal (corresponding to 3 to 4 40x view fields) using Image J (version 2.0.0-rc-39/1.50b). Grey scale images were thresholded and hormone+ and DAPI+ particles ≥ 3.2 μm^2 were measured.

RNA-isolation and cDNA synthesis

Liver, brain, kidney and testis RNA were isolated by guanidine hydrochloride extraction and differential precipitation as described previously (Thomas and Dziadek, 1993). Pituitary gland RNA was isolated using an RNeasy mini kit (Qiagen) as per the manufacturer's instructions. RNA quality was assayed using the Agilent 2100 Bioanalyzer or the Agilent 4200 Tapestation and samples with an RNA integrity number less than 7 were not used for analysis. cDNA synthesis was performed using Superscript III (18080-085, Invitrogen) according to the manufacturer's instructions.

Northern blot

10 µg of RNA was denatured in RNA loading buffer (200 µL 10 x MOPS buffer (pH 7.0), 350 µL formaldehyde, 1000 µL formamide) at 55°C for 15 min. Samples were loaded with 2 µl of gel loading dye (50% (v/v) glycerol, 1 mM EDTA (pH 8.0), 0.25% bromophenol blue and 0.2% xyan cyanol in MQ-H_2O) and separated by gel electrophoresis (1% ultra-pure agarose, 18% formaldehyde, 10% MOPS buffer, recirculating) at 40 V overnight. Following separation, the gel was washed, then stained in 0.5 µg/mL ethidium bromide. The gel was de-stained in dH_2O then photographed using an ultra-violet trans-illuminator. RNA was transferred to a Hybond-N nylon membrane (Amersham Pharmacia Biotech) overnight, dried in an oven at 80°C for 1 h and cross-linked with 50 mJ of UV-light using the GS gene

linker (Bio-Rad, Hercules). A *Phf6* cDNA template corresponding to a region within exon 11, bases 2377 to 3156 of the published *Phf6* sequence (GenBank Accession No. NM_027642) was incubated with *in vitro* DNA polymerase reagents (Megaprime DNA Labelling System, Amersham Biosciences) and ^{32}P-dCTP (EasyTides, PerkinElmer). Synthesised radiolabelled probes were added to 10 ml of preheated hybridization buffer and incubated with the nylon membrane at 65°C overnight. After washing steps the membrane was exposed to X-ray film for 7 days at –70°C.

qPCR

Genomic DNA or cDNA was added to 10 μL, SensiMix SYBR (Bioline Reagents), 10 pmol each of a forward and reverse primer (Table S3 and Table S4) designed using Primer3 (Koressaar and Remm, 2007; Untergasser et al., 2012), and 6 μL MilliQ-H_2O in a LightCycler 480 384-well Plate (Roche). Data were acquired on the LightCycler 480 (Roche) under the following conditions: 95°C for 10 min, x1; 95°C for 20s, 60°C for 20s, 72°C for 30s for 40 cycles. Standard curves based on arbitrary units corresponding to the Cp values obtained from serially diluted standard samples were used to calculate the initial concentration of the unknown samples. All samples were assayed in technical triplicates which were averaged prior to normalization with housekeeping gene(s); *B2m* for genomic DNA, and *Gapdh* and/or *Pgk1* for RT-qPCR. A triplicate measurement was excluded in the rare case where there was a greater than 20% difference compared to the other two replicates for a particular sample (and the average of the other two replicates only was used for analysis).

Skeletal preparations

Skeletal preparations were performed as previously described (Voss et al., 2009), using a protocol adapted from Kaufman et al. (Kaufman, 1992). Specifically, adult carcasses were skinned, fixed in EtOH for 7 days, followed by acetone for 7 days. Subsequently, specimens were stained for 10 days in a solution containing 1 vol of 0.4% alcian blue in 70% EtOH, 1 vol of glacial acetic acid, 14 vol of 95% EtOH, 4 vol of H_2O, and 0.2 vol of 0.5% alizarin red S in H_2O. Samples were rinsed, then kept in a solution of 20% glycerol and 1% potassium hydroxide for 3 days at 37°C, then for 4 days at room temperature. Skeletons were transferred to 50% glycerol prior to imaging and femur length quantification.

Statistical analysis

Statistical analysis including T-tests, Chi-squared tests and ANOVA were performed using Prism 8.

Author Contributions

Conceptualization: AKV, TT; Formal analysis, HMM, AKV; Investigation: HMM, SE, LW; Resources: JG, WSA; Data curation: HMM; Writing – original draft preparation: HMM; Writing – review & editing: AKV, TT, JG, WSA; Visualization: HMM; Supervision: AKV, TT; Project administration: HMM; Funding acquisition: AKV, TT.

Competing Interests

The authors do not have any competing interests to declare.

References

Aasland, R., Gibson, T. J. and Stewart, A. F. (1995). The PHD finger: implications for chromatin-mediated transcriptional regulation. *Trends Biochem Sci* **20**, 56-59.

Abatan, O. I., Welch, K. B. and Nemzek, J. A. (2008). Evaluation of saphenous venipuncture and modified tail-clip blood collection in mice. *J Am Assoc Lab Anim Sci* **47**, 8-15.

Abuzzahab, M. J., Schneider, A., Goddard, A., Grigorescu, F., Lautier, C., Keller, E., Kiess, W., Klammt, J., Kratzsch, J., Osgood, D., et al. (2003). IGF-I receptor mutations resulting in intrauterine and postnatal growth retardation. *N Engl J Med* **349**, 2211-2222.

Alba, M. and Salvatori, R. (2004). A mouse with targeted ablation of the growth hormone-releasing hormone gene: a new model of isolated growth hormone deficiency. *Endocrinology* **145**, 4134-4143.

Allen, D. B. (2006). Growth hormone therapy for short stature: is the benefit worth the burden? *Pediatrics* **118**, 343-348.

Allen, D. B., Rundle, A. C., Graves, D. A. and Blethen, S. L. (1997). Risk of leukemia in children treated with human growth hormone: review and reanalysis. *J Pediatr* **131**, S32-36.

Ardinger, H. H., Hanson, J. W. and Zellweger, H. U. (1984). Borjeson-Forssman-Lehmann syndrome: further delineation in five cases. *Am J Med Genet* **19**, 653-664.

Baker, J., Liu, J. P., Robertson, E. J. and Efstratiadis, A. (1993). Role of insulin-like growth factors in embryonic and postnatal growth. *Cell* **75**, 73-82.

Barinaga, M., Yamonoto, G., Rivier, C., Vale, W., Evans, R. and Rosenfeld, M. G. (1983). Transcriptional regulation of growth hormone gene expression by growth hormone-releasing factor. *Nature* **306**, 84-85.

Baumstark, A., Lower, K. M., Sinkus, A., Andriuskeviciute, I., Jurkeniene, L., Gecz, J. and Just, W. (2003). Novel PHF6 mutation p.D333del causes Borjeson-Forssman-Lehmann syndrome. *J Med Genet* **40**, e50.

Berland, S., Alme, K., Brendehaug, A., Houge, G. and Hovland, R. (2011). PHF6 Deletions May Cause Borjeson-Forssman-Lehmann Syndrome in Females. *Mol Syndromol* **1**, 294-300.

Bernard, V., Young, J. and Binart, N. (2019). Prolactin - a pleiotropic factor in health and disease. *Nat Rev Endocrinol* **15**, 356-365.

Bicknell, L. S., Bongers, E. M., Leitch, A., Brown, S., Schoots, J., Harley, M. E., Aftimos, S., Al-Aama, J. Y., Bober, M., Brown, P. A., et al. (2011a). Mutations in the pre-replication complex cause Meier-Gorlin syndrome. *Nat Genet* **43**, 356-359.

Bicknell, L. S., Walker, S., Klingseisen, A., Stiff, T., Leitch, A., Kerzendorfer, C., Martin, C. A., Yeyati, P., Al Sanna, N., Bober, M., et al. (2011b). Mutations in ORC1, encoding the largest subunit of the origin recognition complex, cause microcephalic primordial dwarfism resembling Meier-Gorlin syndrome. *Nat Genet* **43**, 350-355.

Birrell, G., Lampe, A., Richmond, S., Bruce, S. N., Gecz, J., Lower, K., Wright, M. and Cheetham, T. D. (2003). Borjeson-Forssman-Lehmann syndrome and multiple pituitary hormone deficiency. *J Pediatr Endocrinol Metab* **16**, 1295-1300.

Borjeson, M., Lehmann, O. and Forssman, H. (1962). An X-Linked, Recessively Inherited Syndrome Characterized by Grave Mental Deficiency, Epilepsy, and Endocrine Disorder. *Acta Med Scand* **171**, 13-21.

Carter, M. T., Picketts, D. J., Hunter, A. G. and Graham, G. E. (2009). Further Clinical Delineation of the Borjeson-Forssman-Lehmann Syndrome in Patients with PHF6 Mutations. *Am J Med Genet* **149A**, 246-250.

Chao, M. M., Todd, M. A., Kontny, U., Neas, K., Sullivan, M. J., Hunter, A. G., Picketts, D. J. and Kratz, C. P. (2010). T-Cell Acute Lymphoblastic Leukemia in Association With Borjeson-Forssman-Lehmann Syndrome Due To a Mutation in PHF6. *Pediatr Blood Cancer* **55**, 722-724.

Cheng, C., Deng, P. Y., Ikeuchi, Y., Yuede, C., Li, D., Rensing, N., Huang, J., Baldridge, D., Maloney, S. E., Dougherty, J. D., et al. (2018). Characterization of a Mouse Model of Borjeson-Forssman-Lehmann Syndrome. *Cell Rep* **25**, 1404-1414 e1406.

Chrousos, G. P., Kino, T. and Charmandari, E. (2009). Evaluation of the hypothalamic-pituitary-adrenal axis function in childhood and adolescence. *Neuroimmunomodulation* **16**, 272-283.

Coggeshall, R. E. (1992). A consideration of neural counting methods. *Trends Neurosci* **15**, 9-13.

Crawford, J., Lower, K. M., Hennekam, R. C. M., Van Esch, H., Megarbane, A., Lynch, S. A., Turner, G. and Gecz, J. (2006). Mutation screening in Borjeson-Forssman-Lehmann syndrome: identification of a novel de novo PHF6 mutation in a female patient. *J Med Genet* **43**, 238-243.

de Winter, C. F., van Dijk, F., Stolker, J. J. and Hennekam, R. C. (2009). Behavioural phenotype in Borjeson-Forssman-Lehmann syndrome. *J Intellect Disabil Res* **53**, 319-328.

Declercq, J., Brouwers, B., Pruniau, V. P., Stijnen, P., de Faudeur, G., Tuand, K., Meulemans, S., Serneels, L., Schraenen, A., Schuit, F., et al. (2015). Metabolic and Behavioural Phenotypes in Nestin-Cre Mice Are Caused by Hypothalamic Expression of Human Growth Hormone. *PLoS One* **10**, e0135502.

Dereymaeker, A. M., Fryns, J. P., Hoefnagels, M., Heremans, G., Marien, J. and van den Berghe, H. (1986). The Borjeson-Forssman-Lehmann syndrome. A family study. *Clin Genet* **29**, 317-320.

Eicher, E. M. and Beamer, W. G. (1976). Inherited ateliotic dwarfism in mice. Characteristics of the mutation, little, on chromosome 6. *J Hered* **67**, 87-91.

Favre, H., Benhamou, A., Finidori, J., Kelly, P. A. and Edery, M. (1999). Dual effects of suppressor of cytokine signaling (SOCS-2) on growth hormone signal transduction. *FEBS Lett* **453**, 63-66.

Galichet, C., Lovell-Badge, R. and Rizzoti, K. (2010). Nestin-Cre mice are affected by hypopituitarism, which is not due to significant activity of the transgene in the pituitary gland. *PLoS One* **5**, e11443.

Gan, L., Sun, J., Yang, S., Zhang, X., Chen, W., Sun, Y., Wu, X., Cheng, C., Yuan, J., Li, A., et al. (2020). Chromatin-Binding Protein PHF6 Regulates Activity-Dependent Transcriptional Networks to Promote Hunger Response. *Cell Rep* **30**, 3717-3728 e3716.

Gecz, J., Turner, G., Nelson, J. and Partington, M. (2006). The Borjeson-Forssman-Lehman syndrome (BFLS, MIM #301900). *Eur J Hum Genet* **14**, 1233-1237.

Grasgruber, P., Cacek, J., Kalina, T. and Sebera, M. (2014). The role of nutrition and genetics as key determinants of the positive height trend. *Econ Hum Biol* **15**, 81-100.

Greenhalgh, C. J., Rico-Bautista, E., Lorentzon, M., Thaus, A. L., Morgan, P. O., Willson, T. A., Zervoudakis, P., Metcalf, D., Street, I., Nicola, N. A., et al. (2005). SOCS2 negatively regulates growth hormone action in vitro and in vivo. *J Clin Invest* **115**, 397-406.

Griffith, E., Walker, S., Martin, C. A., Vagnarelli, P., Stiff, T., Vernay, B., Al Sanna, N., Saggar, A., Hamel, B., Earnshaw, W. C., et al. (2008). Mutations in pericentrin cause Seckel syndrome with defective ATR-dependent DNA damage signaling. *Nat Genet* **40**, 232-236.

Grunauer, M. and Jorge, A. A. L. (2018). Genetic short stature. *Growth Horm IGF Res* **38**, 29-33.

Guernsey, D. L., Matsuoka, M., Jiang, H., Evans, S., Macgillivray, C., Nightingale, M., Perry, S., Ferguson, M., LeBlanc, M., Paquette, J., et al. (2011). Mutations in origin recognition complex gene ORC4 cause Meier-Gorlin syndrome. *Nat Genet* **43**, 360-364.

Hsu, Y. C., Chen, T. C., Lin, C. C., Yuan, C. T., Hsu, C. L., Hou, H. A., Kao, C. J., Chuang, P. H., Chen, Y. R., Chou, W. C., et al. (2019). Phf6-null hematopoietic stem cells have enhanced self-renewal capacity and oncogenic potentials. *Blood Adv* **3**, 2355-2367.

Ikegami, K. and Yoshimura, T. (2017). The hypothalamic-pituitary-thyroid axis and biological rhythms: The discovery of TSH's unexpected role using animal models. *Best Pract Res Clin Endocrinol Metab* **31**, 475-485.

Jansen, S., Hoischen, A., Coe, B. P., Carvill, G. L., Van Esch, H., Bosch, D. G. M., Andersen, U. A., Baker, C., Bauters, M., Bernier, R. A., et al. (2018). A genotype-first approach identifies an intellectual disability-overweight syndrome caused by PHIP haploinsufficiency. *Eur J Hum Genet* **26**, 54-63.

Johnson, M. L., Pipes, L., Veldhuis, P. P., Farhy, L. S., Boyd, D. G. and Evans, W. S. (2008). AutoDecon, a deconvolution algorithm for identification and characterization of luteinizing hormone secretory bursts: description and validation using synthetic data. *Anal Biochem* **381**, 8-17.

Johnson, M. L., Pipes, L., Veldhuis, P. P., Farhy, L. S., Nass, R., Thorner, M. O. and Evans, W. S. (2009). AutoDecon: a robust numerical method for the quantification of pulsatile events. *Methods Enzymol* **454**, 367-404.

Kaufman, M. H. (1992). *The Atlas of Mouse Development*: Elsevier.

Klingseisen, A. and Jackson, A. P. (2011). Mechanisms and pathways of growth failure in primordial dwarfism. *Genes Dev* **25**, 2011-2024.

Koressaar, T. and Remm, M. (2007). Enhancements and modifications of primer design program Primer3. *Bioinformatics* **23**, 1289-1291.

Lango Allen, H., Estrada, K., Lettre, G., Berndt, S. I., Weedon, M. N., Rivadeneira, F., Willer, C. J., Jackson, A. U., Vedantam, S., Raychaudhuri, S., et al. (2010). Hundreds of variants clustered in genomic loci and biological pathways affect human height. *Nature* **467**, 832-838.

Li, S., Francisco, A. B., Han, C., Pattabiraman, S., Foote, M. R., Giesy, S. L., Wang, C., Schimenti, J. C., Boisclair, Y. R. and Long, Q. (2010). The full-length isoform of the mouse pleckstrin homology domain-interacting protein (PHIP) is required for postnatal growth. *FEBS Lett* **584**, 4121-4127.

Linossi, E. M., Babon, J. J., Hilton, D. J. and Nicholson, S. E. (2013). Suppression of cytokine signaling: the SOCS perspective. *Cytokine Growth Factor Rev* **24**, 241-248.

Liu, J. P., Baker, J., Perkins, A. S., Robertson, E. J. and Efstratiadis, A. (1993). Mice carrying null mutations of the genes encoding insulin-like growth factor I (Igf-1) and type 1 IGF receptor (Igf1r). *Cell* **75**, 59-72.

Lower, K. M., Turner, G., Kerr, B. A., Mathews, K. D., Shaw, M. A., Gedeon, A. K., Schelley, S., Hoyme, H. E., White, S. M., Delatycki, M. B., et al. (2002). Mutations in PHF6 are associated with Borjeson-Forssman-Lehmann syndrome. *Nat Genet* **32**, 661-665.

Lupu, F., Terwilliger, J. D., Lee, K., Segre, G. V. and Efstratiadis, A. (2001). Roles of Growth Hormone and Insulin-like Growth Factor 1 in Mouse Postnatal Growth. *Dev Biol* **229**, 141-162.

Matsuo, K., Murano, I. and Kajii, T. (1984). Borjeson-Forssman-Lehmann syndrome in a girl. *Jap J Hum Genet* **29**, 121-126.

McRae, H. M., Garnham, A. L., Hu, Y., Witkowski, M. T., Corbett, M. A., Dixon, M. P., May, R. E., Sheikh, B. N., Chiang, W., Kueh, A. J., et al. (2019). PHF6 regulates hematopoietic stem and progenitor cells and its loss synergizes with expression of TLX3 to cause leukemia. *Blood* **133**, 1729-1741.

Metcalf, D., Greenhalgh, C. J., Viney, E., Willson, T. A., Starr, R., Nicola, N. A., Hilton, D. J. and Alexander, W. S. (2000). Gigantism in mice lacking suppressor of cytokine signalling-2. *Nature* **405**, 1069-1073.

Meyer, C. W., Korthaus, D., Jagla, W., Cornali, E., Grosse, J., Fuchs, H., Klingenspor, M., Roemheld, S., Tschop, M., Heldmaier, G., et al. (2004). A novel missense mutation in the mouse growth hormone gene causes semidominant dwarfism, hyperghrelinemia, and obesity. *Endocrinology* **145**, 2531-2541.

Miyagi, S., Sroczynska, P., Kato, Y., Nakajima-Takagi, Y., Oshima, M., Rizq, O., Takayama, N., Saraya, A., Mizuno, S., Sugiyama, F., et al. (2019). The chromatin-binding protein Phf6 restricts the self-renewal of hematopoietic stem cells. *Blood* **133**, 2495-2506.

Morgan, M. A. J., Rickels, R. A., Collings, C. K., He, X., Cao, K., Herz, H. M., Cozzolino, K. A., Abshiru, N. A., Marshall, S. A., Rendleman, E. J., et al. (2017). A cryptic Tudor domain links BRWD2/PHIP to COMPASS-mediated histone H3K4 methylation. *Genes Dev* **31**, 2003-2014.

Nishi, Y., Tanaka, T., Takano, K., Fujieda, K., Igarashi, Y., Hanew, K., Hirano, T., Yokoya, S., Tachibana, K., Saito, T., et al. (1999). Recent status in the occurrence of leukemia in growth hormone-treated patients in Japan. GH Treatment Study Committee of the Foundation for Growth Science, Japan. *J Clin Endocrinol Metab* **84**, 1961-1965.

Oh, S., Boo, K., Kim, J., Baek, S. A., Jeon, Y., You, J., Lee, H., Choi, H. J., Park, D., Lee, J. M., et al. (2020). The chromatin-binding protein PHF6 functions as an E3 ubiquitin ligase of H2BK120 via H2BK12Ac recognition for activation of trophectodermal genes. *Nucleic Acids Res*.

Perkins, J. M., Subramanian, S. V., Davey Smith, G. and Ozaltin, E. (2016). Adult height, nutrition, and population health. *Nutr Rev* **74**, 149-165.

Petridou, M., Kimiskidis, V., Deligiannis, K. and Kazis, A. (1997). Borjeson-Forssman-Lehmann syndrome: two severely handicapped females in a family. *Clin Neurol Neurosurg* **99**, 148-150.

Pfaffle, R. and Klammt, J. (2011). Pituitary transcription factors in the aetiology of combined pituitary hormone deficiency. *Best Pract Res Clin Endocrinol Metab* **25**, 43-60.

Phelps, C. J., Dalcik, H., Endo, H., Talamantes, F. and Hurley, D. L. (1993). Growth hormone-releasing hormone peptide and mRNA are overexpressed in GH-deficient Ames dwarf mice. *Endocrinology* **133**, 3034-3037.

Phillips, S. A., Rotman-Pikielny, P., Lazar, J., Ando, S., Hauser, P., Skarulis, M. C., Brucker-Davis, F. and Yen, P. M. (2001). Extreme thyroid hormone resistance in a patient with a novel truncated TR mutant. *J Clin Endocrinol Metab* **86**, 5142-5147.

Podcheko, A., Northcott, P., Bikopoulos, G., Lee, A., Bommareddi, S. R., Kushner, J. A., Farhang-Fallah, J. and Rozakis-Adcock, M. (2007). Identification of a WD40 repeat-containing isoform of PHIP as a novel regulator of beta-cell growth and survival. *Mol Cell Biol* **27**, 6484-6496.

Powell-Braxton, L., Hollingshead, P., Warburton, C., Dowd, M., Pitts-Meek, S., Dalton, D., Gillett, N. and Stewart, T. A. (1993). IGF-I is required for normal embryonic growth in mice. *Genes Dev* **7**, 2609-2617.

Pugliese-Pires, P. N., Fortin, J. P., Arthur, T., Latronico, A. C., Mendonca, B. B., Villares, S. M., Arnhold, I. J., Kopin, A. S. and Jorge, A. A. (2011). Novel inactivating mutations in the GH secretagogue receptor gene in patients with constitutional delay of growth and puberty. *Eur J Endocrinol* **165**, 233-241.

Radcliffe, D. J., Pliskin, J. S., Silvers, J. B. and Cuttler, L. (2004). Growth hormone therapy and quality of life in adults and children. *Pharmacoeconomics* **22**, 499-524.

Ranke, M. B. and Wit, J. M. (2018). Growth hormone - past, present and future. *Nat Rev Endocrinol* **14**, 285-300.

Rauch, A., Thiel, C. T., Schindler, D., Wick, U., Crow, Y. J., Ekici, A. B., van Essen, A. J., Goecke, T. O., Al-Gazali, L., Chrzanowska, K. H., et al. (2008). Mutations in the pericentrin (PCNT) gene cause primordial dwarfism. *Science* **319**, 816-819.

Rico-Bautista, E., Flores-Morales, A. and Fernandez-Perez, L. (2006). Suppressor of cytokine signaling (SOCS) 2, a protein with multiple functions. *Cytokine Growth Factor Rev* **17**, 431-439.

Robinson, L. K., Jones, K. L., Culler, F., Nyhan, W. L., Sakati, N. and Jones, K. L. (1983). The Borjeson-Forssman-Lehmann syndrome. *Am J Med Genet* **15**, 457-468.

Schwenk, F., Baron, U. and Rajewsky, K. (1995). A cre-transgenic mouse strain for the ubiquitous deletion of loxP-flanked gene segments including deletion in germ cells. *Nucleic Acids Res* **23**, 5080-5081.

Soto-Feliciano, Y. M., Bartlebaugh, J. M. E., Liu, Y. P., Sanchez-Rivera, F. J., Bhutkar, A., Weintraub, A. S., Buenrostro, J. D., Cheng, C. S., Regev, A., Jacks, T. E., et al. (2017). PHF6 regulates phenotypic plasticity through chromatin organization within lineage-specific genes. *Genes Dev* **31**, 973-989.

Stamatiades, G. A. and Kaiser, U. B. (2018). Gonadotropin regulation by pulsatile GnRH: Signaling and gene expression. *Mol Cell Endocrinol* **463**, 131-141.

Steyn, F. J., Huang, L., Ngo, S. T., Leong, J. W., Tan, H. Y., Xie, T. Y., Parlow, A. F., Veldhuis, J. D., Waters, M. J. and Chen, C. (2011). Development of a method for the determination of pulsatile growth hormone secretion in mice. *Endocrinology* **152**, 3165-3171.

Steyn, F. J., Wan, Y., Clarkson, J., Veldhuis, J. D., Herbison, A. E. and Chen, C. (2013). Development of a methodology for and assessment of pulsatile luteinizing hormone secretion in juvenile and adult male mice. *Endocrinology* **154**, 4939-4945.

Stochholm, K. and Kiess, W. (2018). Long-term safety of growth hormone-A combined registry analysis. *Clin Endocrinol* **88**, 515-528.

Thackray, V. G., Mellon, P. L. and Coss, D. (2010). Hormones in synergy: regulation of the pituitary gonadotropin genes. *Mol Cell Endocrinol* **314**, 192-203.

Thomas, T., Corcoran, L. M., Gugasyan, R., Dixon, M. P., Brodnicki, T., Nutt, S. L., Metcalf, D. and Voss, A. K. (2006). Monocytic leukemia zinc finger protein is essential for the development of long-term reconstituting hematopoietic stem cells. *Genes Dev* **20**, 1175-1186.

Thomas, T. and Dziadek, M. (1993). Capacity to form choroid plexus-like cells in vitro is restricted to specific regions of the mouse neural ectoderm. *Development* **117**, 253-262.

Todd, M. A. M. and Picketts, D. J. (2012). PHF6 Interacts with the Nucleosome Remodeling and Deacetylation (NuRD) Complex. *J Proteome Res* **11**, 4326-4337.

Tronche, F., Kellendonk, C., Kretz, O., Gass, P., Anlag, K., Orban, P. C., Bock, R., Klein, R. and Schutz, G. (1999). Disruption of the glucocorticoid receptor gene in the nervous system results in reduced anxiety. *Nat Genet* **23**, 99-103.

Turner, G., Gedeon, A., Mulley, J., Sutherland, G., Rae, J., Power, K. and Arthur, I. (1989). Borjeson-Forssman-Lehmann syndrome: clinical manifestations and gene localization to Xq26-27. *Am J Med Genet* **34**, 463-469.

Turner, G., Lower, K. M., White, S. M., Delatycki, M., Lampe, A. K., Wright, M., Clayton-Smith, J., Kerr, B., Schelley, S., Hoyme, H. E., et al. (2004). The clinical picture of the Borjeson-Forssman-Lehmann syndrome in males and heterozygous females with PHF6 mutations. *Clinical Genetics* **65**, 226-232.

Untergasser, A., Cutcutache, I., Koressaar, T., Ye, J., Faircloth, B. C., Remm, M. and Rozen, S. G. (2012). Primer3--new capabilities and interfaces. *Nucleic Acids Res* **40**, e115.

Van Vlierberghe, P., Palomero, T., Khiabanian, H., Van der Meulen, J., Castillo, M., Van Roy, N., De Moerloose, B., Philippe, J., Gonzalez-Garcia, S., Toribio, M. L., et al. (2010). PHF6 mutations in T-cell acute lymphoblastic leukemia. *Nat Genet* **42**, 338-342.

Van Vlierberghe, P., Patel, J., Abdel-Wahab, O., Lobry, C., Hedvat, C. V., Balbin, M., Nicolas, C., Payer, A. R., Fernandez, H. F., Tallman, M. S., et al. (2011). PHF6 mutations in adult acute myeloid leukemia. *Leukemia* **25**, 130-134.

Voss, A. K., Collin, C., Dixon, M. P. and Thomas, T. (2009). Moz and retinoic acid coordinately regulate H3K9 acetylation, Hox gene expression, and segment identity. *Dev Cell* **17**, 674-686.

Voss, A. K., Gamble, R., Collin, C., Shoubridge, C., Corbett, M., Gecz, J. and Thomas, T. (2007). Protein and gene expression analysis of Phf6, the gene mutated in the Borjeson-Forssman-Lehmann Syndrome of intellectual disability and obesity. *Gene Expr Patterns* **7**, 858-871.

Wajnrajch, M. P., Gertner, J. M., Harbison, M. D., Chua, S. C., Jr. and Leibel, R. L. (1996). Nonsense mutation in the human growth hormone-releasing hormone receptor causes growth failure analogous to the little (lit) mouse. *Nat Genet* **12**, 88-90.

Warmerdam, D. O., Alonso-de Vega, I., Wiegant, W. W., van den Broek, B., Rother, M. B., Wolthuis, R. M., Freire, R., van Attikum, H., Medema, R. H. and Smits, V. A. (2020). PHF6 promotes non-homologous end joining and G2 checkpoint recovery. *EMBO Rep* **21**, e48460.

Watanabe, S., Mizuno, S., Oshima, L. H., Tsunematsu, Y., Fujimoto, J. and Komiyama, A. (1993). Leukemia and other malignancies among GH users. *J Pediatr Endocrinol* **6**, 99-108.

Watanabe, S., Tsunematsu, Y. and Fujimoto, J. (1988). Leukaemia in patients treated with growth hormone. *Lancet* **1**, 1159-1160.

Weber, F. T., Frias, J. L., Julius, R. L. and Felman, A. H. (1978). Primary hypogonadism in the Borjeson-Forssman-Lehmann syndrome. *J Med Genet* **15**, 63-66.

Webster, E., Cho, M. T., Alexander, N., Desai, S., Naidu, S., Bekheirnia, M. R., Lewis, A., Retterer, K., Juusola, J. and Chung, W. K. (2016). De novo PHIP-predicted deleterious variants are associated with developmental delay, intellectual disability, obesity, and dysmorphic features. *Cold Spring Harb Mol Case Stud* **2**, a001172.

Wendorff, A. A., Quinn, S. A., Rashkovan, M., Madubata, C. J., Ambesi-Impiombato, A., Litzow, M. R., Tallman, M. S., Paietta, E., Paganin, M., Basso, G., et al. (2019). Phf6 Loss Enhances HSC Self-Renewal Driving Tumor Initiation and Leukemia Stem Cell Activity in T-ALL. *Cancer Discov* **9**, 436-451.

Wit, J. M., Oostdijk, W., Losekoot, M., van Duyvenvoorde, H. A., Ruivenkamp, C. A. and Kant, S. G. (2016). Mechanisms In Endocrinology: Novel genetic causes of short stature. *Eur J Endocrinol* **174**, R145-173.

Zhang, X., Fan, Y., Liu, X., Ang Zhu, M., Sun, Y., Yan, H., He, Y., Ye, X., Gu, X. and Yu, Y. (2019). A Novel Nonsense Mutation of PHF6 in a Female with Extended Phenotypes of Borjeson-Forssman-Lehmann Syndrome. *J Clin Res Pediatr Endocrinol*. 11(4):419-425.

Zhou, Y., Xu, B. C., Maheshwari, H. G., He, L., Reed, M., Lozykowski, M., Okada, S., Cataldo, L., Coschigamo, K., Wagner, T. E., et al. (1997). A mammalian model for Laron syndrome produced by targeted disruption of the mouse growth hormone receptor/binding protein gene (the Laron mouse). *Proc Natl Acad Sci* **94**, 13215-13220.

Zweier, C., Kraus, C., Brueton, L., Cole, T., Degenhardt, F., Engels, H., Gillessen-Kaesbach, G., Graul-Neumann, L., Horn, D., Hoyer, J., et al. (2013). A new face of Borjeson-Forssman-Lehmann syndrome? De novo mutations in PHF6 in seven females with a distinct phenotype. *J Med Genet* **50**, 838-847.

Table

Table 1: GH secretion parameters

GH secretion analysis*							
Experimental group	*Pair 1*		*Pair 2*		*Pair 3*		
Genotype	*Phf6$^{+/Y}$*	*Phf6$^{-/Y}$*	*Phf6$^{+/Y}$*	*Phf6$^{-/Y}$*	*Phf6$^{+/Y}$*	*Phf6$^{-/Y}$*	P-value
Area under curve	80454	58245	1.92×10^5	1.01×10^5	59739	23094	0.04
Average concentration (pg/mL)	223.48	161.79	532.18	288.24	165.94	64.15	0.04
Basal secretion rate (pg/mL per min)	24.94	4.37	8.21	2.69×10^4	2.99	1.24	0.14
Number peaks	3	4	7	1	6	4	0.20
Sum peak mass (pg)	13791.3	3212.3	3.60×10^4	517.38	3501.16	817.51	0.06
Maximum peak mass (pg)	8955.9	1415.6	6144.9	517.38	1304.9	398.69	0.02
Average peak mass (pg)	4597.1	803.08	5143.79	517.38	583.53	204.38	0.02

*Analysis of data displayed in Fig. 2A. Secretion parameters were calculated using *AutoDecon*. P-value was determined using a one-tailed paired T-test for each parameter. The area under the curve, the average concentration, the maximum peak mass and the average peak mass were significantly reduced in *Phf6$^{-/Y}$* compared to *Phf6$^{+/Y}$* mice.
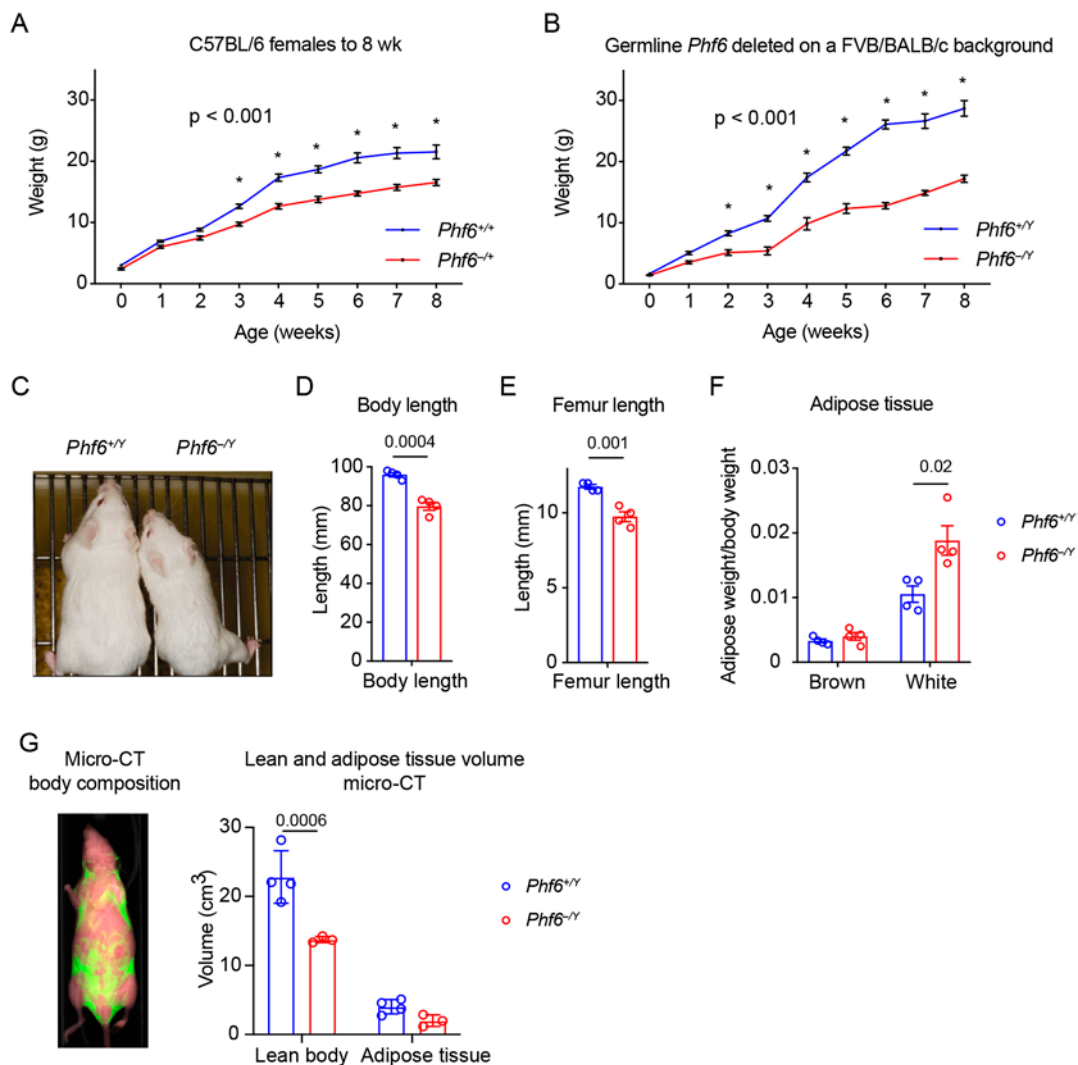
Figures

Figure 1: Germline *Phf6* deletion causes a postnatal growth defect

(A) Heterozygous germline deletion of *Phf6* in females results in reduced overall body weight (C57BL/6 background). n = 7 to 11 animals for each time point.

(B) Hemizygous germline deletion of *Phf6* in males results in reduced overall body weight (FVB/BALB/c background). n = 4 to 16 animals for each time point.

(C) Representatives of *Phf6*$^{+/Y}$ (left) and *Phf6*$^{-/Y}$ (right) mice on the FVB/BALB/c background.

(D) Body length is significantly reduced in *Phf6*$^{-/Y}$ compared to *Phf6*$^{+/Y}$ FVB/BALB/c mice.

(E) Femur length is significantly reduced in $Phf6^{-/Y}$ compared to $Phf6^{+/Y}$ FVB/BALB/c mice.

(F) Brown adipose tissue was isolated from the interscapular region, while white adipose tissue is pooled from the inguinal and dorsal lumbar regions for measurement.

(G) Representative micro-CT image of a wild-type mouse and numerical assessment of the lean body volume and the adipose tissue volume by micro-CT in $Phf6^{-/Y}$ compared to $Phf6^{+/Y}$ FVB/BALB/c mice.

n = 3 - 4 animals per genotype and were 8 to 9 weeks old FVB/BALB/c mice (D-F). Data are presented as mean ± SEM and were analyzed by a two-way ANOVA followed by Bonferroni's post-hoc test for multiple comparisons in A-B. The p-value in A-B indicates results of the overall effect of genotype in the two-way ANOVA analysis, while the asterisks indicate a p-value less than 0.05 in multiple comparison tests.

Data points in D-G represent results of individual animals, with mean ± SEM. Data in D-G were analysed by a two-tailed Student's T-test.
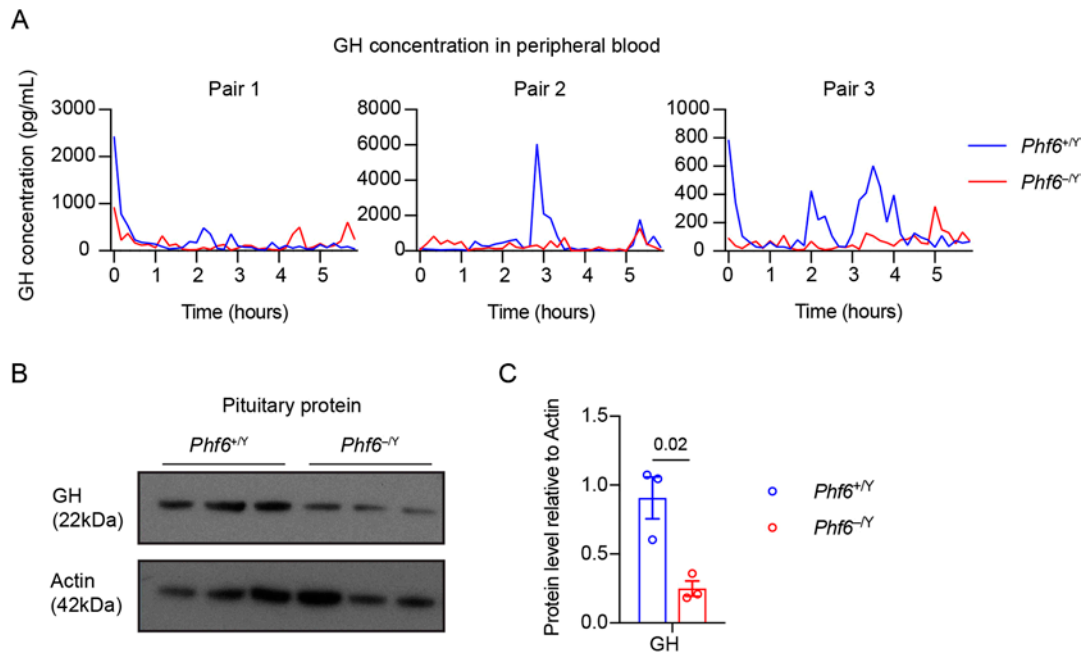
Figure 2: Circulating and pituitary GH levels are reduced in *Phf6$^{-/Y}$* mice

(A) GH concentration measured at 10-minute intervals over a 6 hour time period. Analysis of data is presented in Table 1. Each line displays data from one animal (n = 3 animals per genotype).

(B) Western blot showing GH and actin protein levels in pituitary lysates from *Phf6$^{-/Y}$* and *Phf6$^{+/Y}$* mice. Each lane represents protein from an individual animal (n = 3 per genotype).

(C) Quantification of data shown in (B) demonstrating reduced GH protein levels relative to actin protein in the pituitary of *Phf6$^{-/Y}$* compared to *Phf6$^{+/Y}$* mice.

All data in this figure refer to mice on the FVB/BALB/c background. In C, each individual animal is presented as a circle and mean ± SEM are shown. Data were analyzed by a two-tailed Student's T-test.
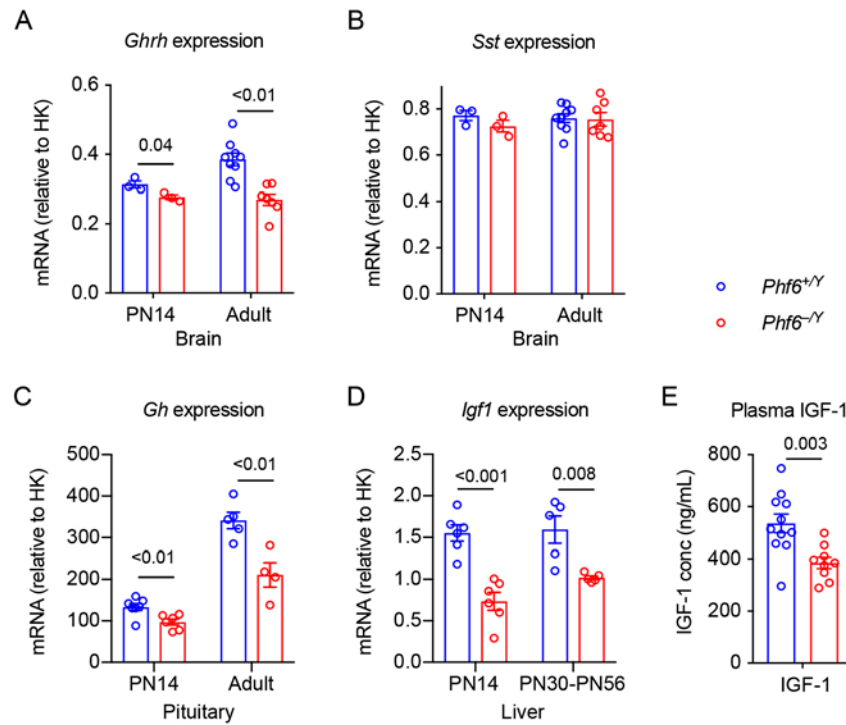
Figure 3: mRNA levels of brain *Sst*, brain *Ghrh*, pituitary *Gh*, and liver *Igf1* in *Phf6*^{–/Y} mice compared to controls

RT-qPCR data are shown.

(A) *Ghrh* mRNA levels in the brain of p14 and adult mice.

(B) *Sst* mRNA levels n in the brain of p14 and adult mice.

(C) *Gh* mRNA levels in pituitaries isolated from p14 and adult mice.

(D) *Igf1* mRNA levels in the liver of p14 and p30-p56 mice.

(E) IGF-1 protein levels in plasma as assessed by ELISA.

Data are presented as mean ± SEM of arbitrary units corresponding to the Cp values and are normalized to housekeeping (HK) genes (*Gapdh* and *Pgk1*). Each data point represents one animal. PN14 = postnatal day 14. Final mRNA values were analyzed by a two-tailed Student's t-test.
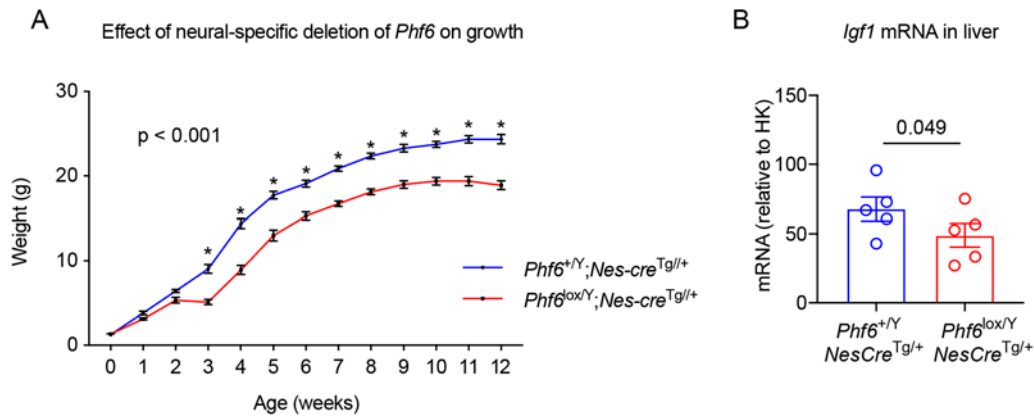
Figure 4: Nervous system specific deletion of *Phf6* causes a postnatal growth defect and a reduction in liver *Igf1* mRNA

(A) Weekly weight of control mice (*Phf6*$^{+/Y}$;*Nes-cre*$^{Tg/+}$, n = 5 to 18 per time point) and mice with *Phf6* deleted in the nervous system (*Phf6*^{loxY};*Nes-cre*$^{Tg/+}$, n = 4 to 14 per time point). Data are presented as mean ± SEM and, at each time point, were analysed by a two-way ANOVA with Bonferroni's post-hoc test for comparisons at each time point. *, p-value less than 0.05 for multiple comparison at that time point. (B) *Igf1* mRNA levels relative to the housekeeping (HK) gene *Gapdh* assessed by RT-qPCR in the livers of 8-12 week-old *Phf6*^{loxY};*Nes-cre*$^{Tg/+}$ and *Phf6*$^{+/Y}$;*Nes-cre*$^{Tg/+}$ control mice. Data are presented as mean ± SEM and were analysed by one-tailed Student's T-test. Each data point represents one animal, n = 5 animals per genotype.
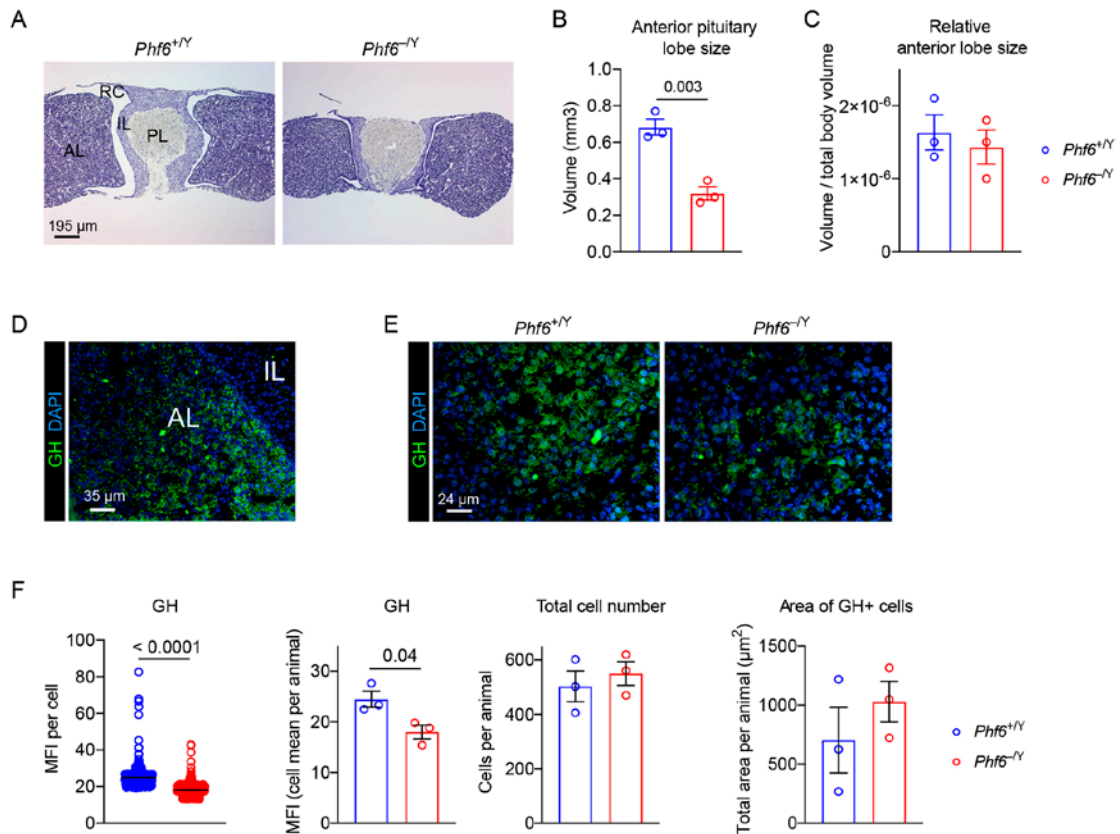
Figure 5: GH levels per cell are reduced in the absence of PHF6

(A) Representative images of cresyl violet-stained horizontal sections of 4-week old *Phf6*$^{+/Y}$ and *Phf6*$^{-/Y}$ pituitary glands.

(B) Assessment of the volumes of the anterior lobes of *Phf6*$^{+/Y}$ and *Phf6*$^{-/Y}$ pituitary glands using the method described by Coggeshall (Coggeshall, 1992).

(C) Volume of the anterior lobe of *Phf6*$^{+/Y}$ and *Phf6*$^{-/Y}$ pituitary glands relative to the total body volume.

(D) Representative GH immunofluorescence image showing the specificity of the antibody detecting GH in the anterior lobe (AL), but not in the intermediate lobe (IL) of the pituitary gland, as expected. GH green; DAPI blue.

(E) Representative higher magnification GH immunofluorescence image of the anterior lobe of the pituitary glands of 6-7 week-old *Phf6*$^{+/Y}$ and *Phf6*$^{-/Y}$ mice.

(F) Numerical assessment of GH immunofluorescence intensity per cell and summarised per animal, as well as total cell number in the tissue area analysed and area of GH+ cells in *Phf6*$^{+/Y}$ and *Phf6*$^{-/Y}$ pituitary glands.

AL, anterior lobe; IL, intermediate lobe; PL, posterior lobe; RC Rathke's cleft.

Data are presented as mean ± SEM and were analysed by one-tailed Student's T-test. n = 3 animals per genotype (B,C,F). Each data point represents one animal (B,C,F), except (F) left panel, where it represents one cell and 402 to 620 cells for each of 3 animals per genotype were assessed.
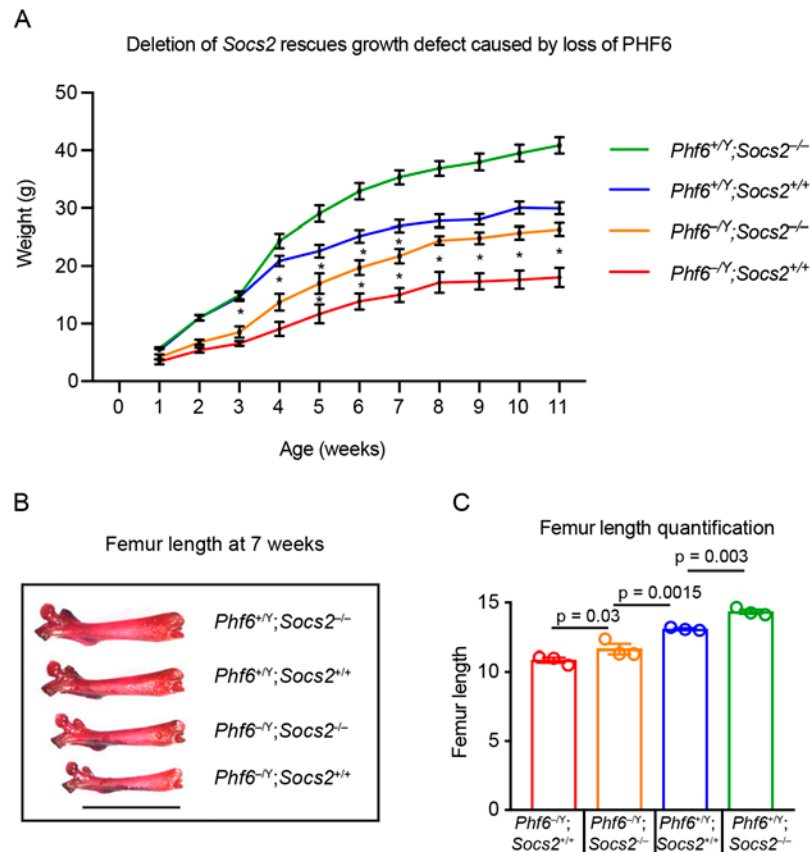
Figure 6: Deletion of *Socs2* rescues the growth defect caused by loss of PHF6

(A) Weekly weight of mice of the indicated genotypes.

Data are presented as mean ± SEM and were analysed by a two-way ANOVA with Bonferroni's post-hoc test for multiple comparisons. * indicates p-value less than 0.05 for multiple-comparisons between genotypes corresponding to lines on either side of the asterisk, only showing results for comparisons between *Phf6*[−/Y];*Socs2*^{+/+} and *Phf6*[−/Y];*Socs2*^{−/−} genotypes and comparisons between *Phf6*[−/Y];*Socs2*^{−/−} and *Phf6*[+/Y];*Socs2*^{+/+} genotypes. Full results from multiple comparison tests are presented in Table S11. n = 4 to 9 animals per genotype.

(B) Representative femurs stained with alizarin red S and alcian blue from mice of the indicated genotype. Scale bar = 10 mm.

(C) Quantification of femur length in mice of the indicated genotype (units are mm). Each individual animal (n = 3 per genotype) is presented as a circle and mean ± SEM are shown. Data are presented as mean ± SEM and were analysed by a one-way ANOVA with Fisher's LSD test for multiple comparisons.
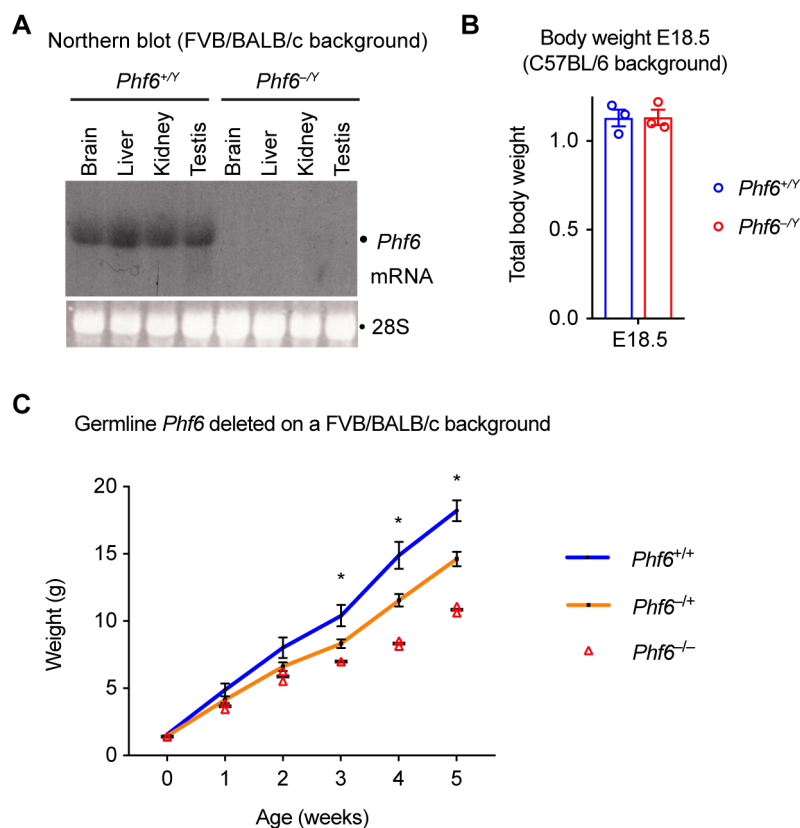
Figure S1: *Phf6* mutation causes reduced body weight

(A) Northern blot showing *Phf6* mRNA (4.5 kb) in organs from *Phf6*$^{+/Y}$ mice, which is not detectable in organs from *Phf6*$^{-/Y}$ mice. 10 µg of total RNA was loaded per lane. Blots were probed with a *Phf6*-specific [^{32}P]dCTP-labeled cDNA probe (corresponding to a region within exon 11, bases 2377 to 3156 of the published sequence, GenBank Accession No. NM_027642) and exposed to film for 7 days. The ethidium bromide-stained 28S rRNA is shown as a loading control.

(B) Body weight of *Phf6*$^{+/Y}$ and *Phf6*$^{-/Y}$ males (C57BL/6 background) at E18.5 showing no difference between genotypes. n = 3 per genotype. Each individual animal is presented as a circle. Data are presented mean ± SEM and were analysed by a two-tailed Student's t-test.

(C) Weekly weights of mice of the indicated genotype on the FVB/BALB/c genetic background. n = 7 *Phf6*$^{+/+}$, n = 14 *Phf6*$^{-/+}$, n = 2 *Phf6*$^{-/-}$. Data are presented mean ± SEM. * Indicates significant results from a comparison between the *Phf6*$^{+/+}$ and the *Phf6*$^{-/+}$ genotypes and *Phf6*$^{+/+}$ and the *Phf6*$^{-/-}$ genotypes as assessed by a two-way ANOVA followed by Bonferroni's post-hoc test.
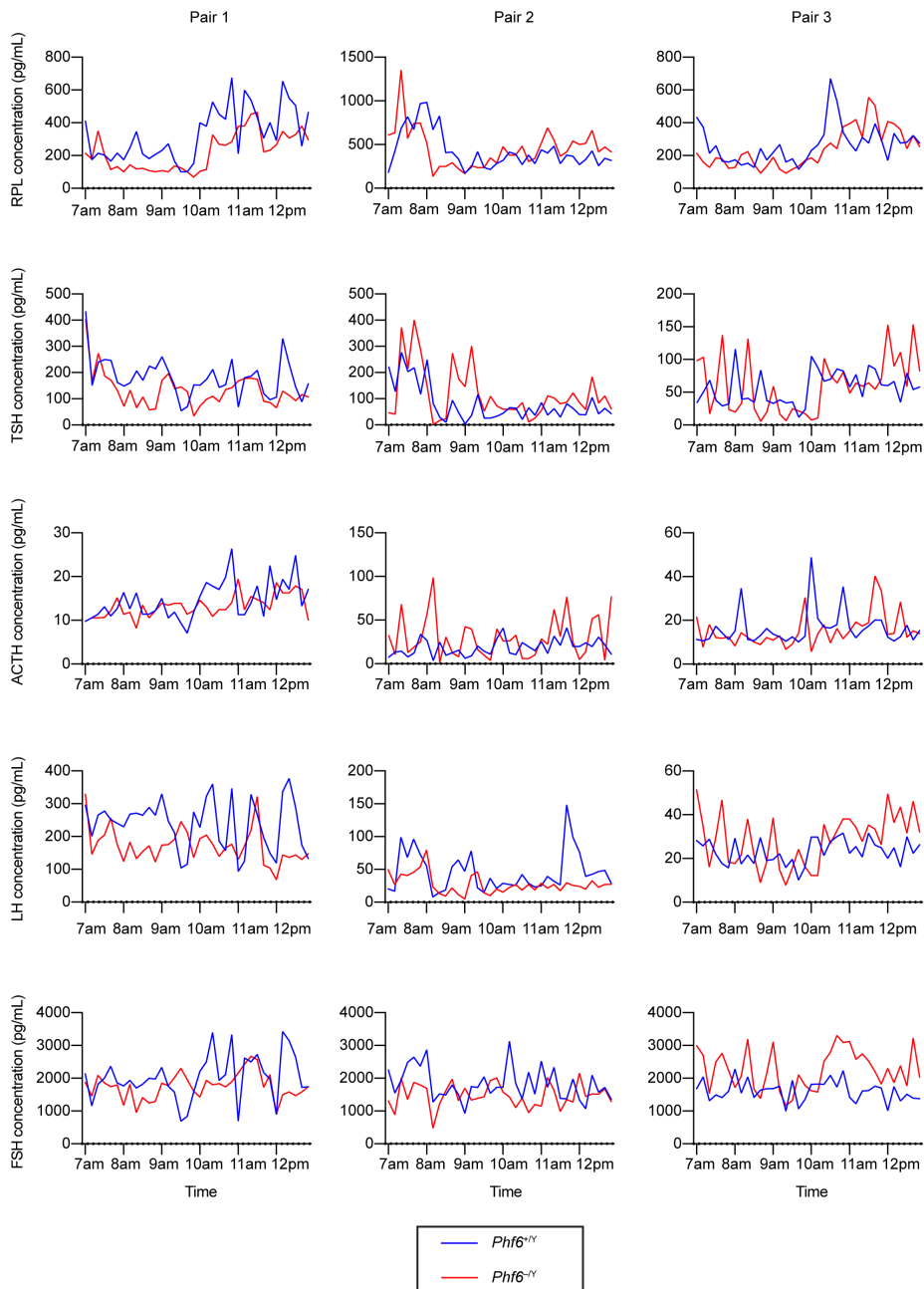
Figure S2: Blood levels of anterior pituitary hormones
Concentrations of the indicated hormones in the peripheral blood analysed at 10-minute intervals over 6 hours. Each experimental pair consisted of one $Phf6^{-/Y}$ and a littermate $Phf6^{+/Y}$ control mouse (n = 3 animals per genotype). Each line represents one animal. Secretion parameters for each hormone are listed in Tables S6-S10 (no significant differences).
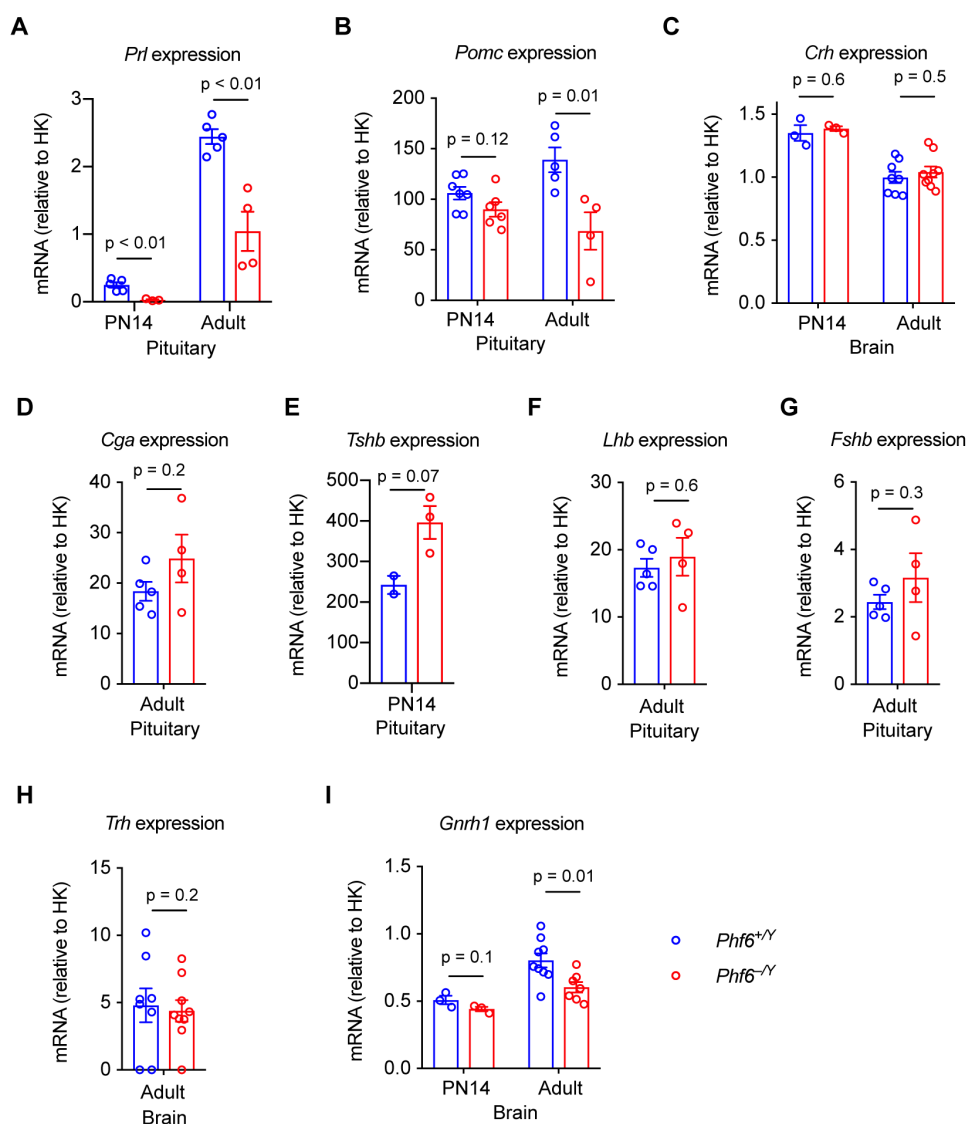
Figure S3: mRNA levels of endocrine genes

mRNA levels of endocrine genes in the pituitary gland and brain as determined by RTqPCR

(A) *Prl* (*prolactin*) mRNA levels in the p14 and adult pituitary gland.

(B) *Pomc* (*pro-opiomelanocortin,* ACTH precursor) mRNA levels in the p14 and adult pituitary gland.

(C) *Crh (corticotropin-releasing hormone*) mRNA levels in the p14 and adult brain.

(D) *Cga* (*chorionic gonadotropin-alpha*)*,* common alpha subunit of TSH, LH, and FSH) mRNA levels in the p14 and adult pituitary.

(E) *Tshb (thyroid stiumulating hormone beta subunit)* mRNA levels in the p14 pituitary gland.

(F) *Lhb* (*luteinizing hormone beta subunit*) mRNA levels in the adult pituitary gland.

(G) *Fshb* (*follicle-stimulating hormone beta subunit*) mRNA levels in the adult pituitary gland.

(H) *Trh* (*thyrotropin releasing hormone)* expression in the adult brain.

(I) *Gnrh1* (*gonadotropin releasing hormone 1*) expression in the p14 and adult brain.

n is indicated by the number of data points representing individual animals. Data are presented as mean ± SEM of arbitrary units corresponding to the Cp values and are normalized to housekeeping (HK) genes (*Gapdh* and/or *Pgk1*). Note that because arbitrary units were used to assign concentrations to the Cp value in standard curves produced from serially diluted samples, the number corresponding to relative mRNA level is not comparable between genes. Data are presented mean ± SEM and analysed by a two-tailed Student's T-test. PN14 = postnatal day 14. Final mRNA values were analyzed by a two-tailed Student's t-test.
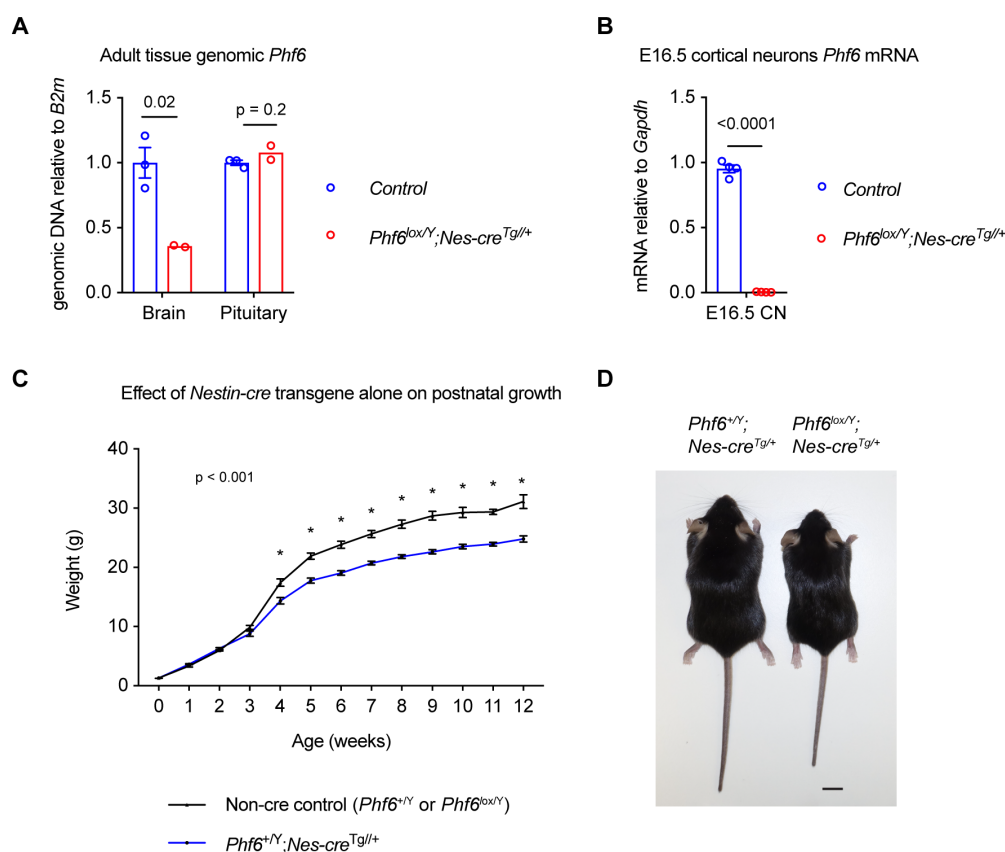
Figure S4: Efficient deletion of *Phf6* in neural tissue, but not the pituitary gland by the *Nestin-cre* transgene (C57BL/6 background)

(A) Genomic qPCR assessment of level of genomic *Phf6* DNA in adult brain tissue and adult pituitary tissue using primers which amplify a region of exon 4 and the intron between exons 4 and 5 (ie. within the deleted region), demonstrating deletion of *Phf6* in the brain, but not in the pituitary gland. Note that adult brain tissue contains non-neural cell types, thus residual *Phf6* DNA is likely derived from non-neural cell types. n = 3 controls (*Phf6*$^{lox/Y}$;*Nes-cre*$^{+/+}$), n = 2 *Phf6*$^{lox/Y}$;*Nes-cre*$^{Tg/+}$.

(B) mRNA expression as assessed by RT-qPCR showing efficient deletion of *Phf6* in a purified population of embryonic day 16.5 (E16.5) *Phf6*$^{lox/Y}$;*Nes-cre*$^{Tg/+}$ cortical neurons (CN). n = 4 controls (*Phf6*$^{+/Y}$;*Nes-cre*$^{Tg/+}$), n = 4 *Phf6*$^{lox/Y}$;*Nes-cre*$^{Tg/+}$.

(C) Growth curve confirming the previously published (Declercq et al., 2015) effects of the *Nestin-cre* transgene alone on postnatal body weight, here showing a significant effect after 4 weeks of age. n = 5 to 18 *Nestin-cre* controls (*Phf6*$^{+/Y}$;*Nes-cre*$^{Tg/+}$) per time point, n = 3 to 12 non-cre controls per time point (9 *Phf6*$^{lox/Y}$, n = 3 *Phf6*$^{+/Y}$).

(D) Photo of representative 6 week old *Phf6*$^{lox/Y}$;*Nes-cre*$^{Tg/+}$ mouse showing proportional reduction in overall body size compared to a littermate control *Phf6*$^{+/Y}$;*Nes-cre*$^{Tg/+}$ mouse. Scale bar = 1 cm.

n is indicated by the number of data points representing individual animals (A,B). Data are presented mean ± SEM and were analysed by a two-tailed Student's t-test for A-B, and a two-way ANOVA for C, with Bonferroni's correction for multiple comparisons.
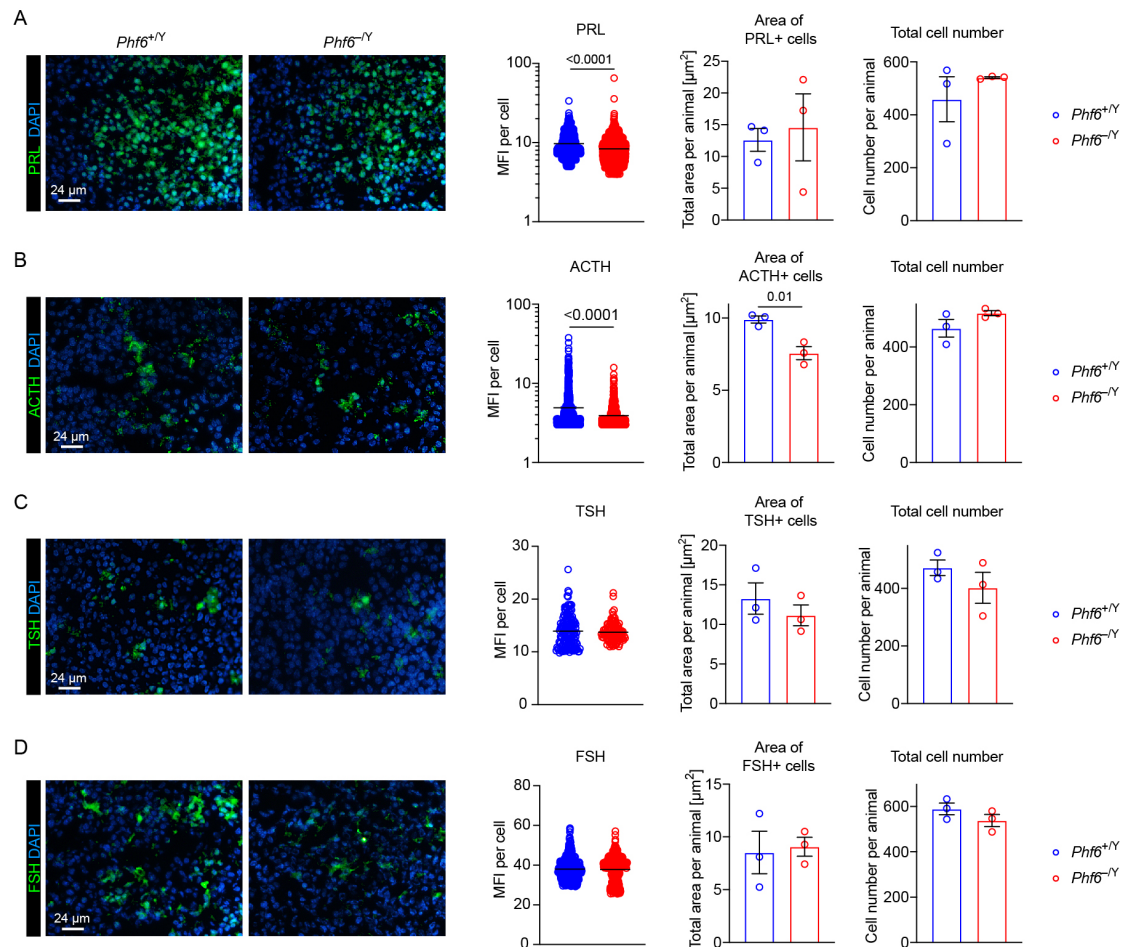
Figure S5: PRL and ACTH levels per cell are reduced in the absence of PHF6
(A) Representative images of PRL immunofluorescence in the anterior lobe of the
pituitary glands of 6-7 week-old *Phf6*$^{+/Y}$ and *Phf6*$^{-/Y}$ mice and numerical assessment
of PRL immunofluorescence intensity per cell, as well as the area of PRL+ cells and
the total cell number in the tissue area analysed in *Phf6*$^{+/Y}$ and *Phf6*$^{-/Y}$ pituitary glands.
(B) Same as (A), but displaying ACTH.
(C) Same as (A), but displaying TSH.
(D) Same as (A), but displaying FSH.
Data are presented as mean ± SEM and were analysed by one-tailed Student's T-test.
n = 3 animals per genotype (A-D). Each data point represents one cell in the left graph
(A-D). Each data point represents one animal in the middle and right graphs (A-D).

Table S1: Table summarizing published endocrine data from BFLS patients

The summary data by Zhang et al. (2019) (Zhang et al., 2019) were adjusted to align them with the data presented in the primary literature based on reports by (Ardinger et al., 1984; Baumstark et al., 2003; Birrell et al., 2003; Carter et al., 2009; Crawford et al., 2006; de Winter et al., 2009; Dereymaeker et al., 1986; Matsuo et al., 1984; Petridou et al., 1997; Robinson et al., 1983; Turner et al., 1989; Weber et al., 1978). Note results from Veall et al. (1979) have been excluded due to later reports that the described case was incorrectly diagnosed as BFLS (Ardinger et al., 1984; Preus, 1984).

Pituitary hormone levels in BFLS patients

	GH	TSH	PRL	ACTH	LH	FSH
Male BLFS	3/4 down	2/4 down	1/1 normal	1-2 down?*	2/16 down, 1/16 up	3/15 down, 4/15 up
Female BFLS	3/4 down	1/5 up	3/3 normal	n.d.	3/5 down	3/5 down

*Birrell et al. 2003 describe in the abstract that ACTH deficiency was identified, however these results are not expanded in the report and it is not clear whether this was found in one or both of the reported patients.

Table S2: Genotyping primers

Gene	Primers (5'-3')
Phf6	TGAAATATAGAGCTGGTCAATCAC
	TACAGTATTTTGGGGAAGCTGG
	ATAATCCGAGATTGAATCTAACCC
Nestin-cre transgene	GCGCGGTCTGGCAGTAAAAAC
	GCAGATGGCGCGGCAACACC
Socs2	GTCACGTTGGTGTAGATGGGCGC
	GGCTCCAGGCACCGCAGGGTCAT
	TGGTACAGAACACGCAGGCGGAGGAGT

Table S3: Genomic qPCR primers

Gene	Forward (5'-3')	Reverse (5'-3')
Phf6	ACCACTGTGCATTGCATGAT	TGACGGTGAAATGCTTTGAA
B2m	TGAACGACCAGATACACCAAAC	AAAGGGACTTTCCCATTTTCAG

Table S4: RTqPCR primers

Gene	Forward (5'-3')	Reverse (5'-3')
Cga	CTGTGTGGCCAAAGCATTTA	GCGCTCAGAAGCTACGACTT
Crh	CACCTACCAAGGGAGGAGAA	CAGGCAGGACGACAGAGC
Fshb	AGAGAAGGAAGAGTGCCGTT	CCGAGCTGGGTCCTTATACA
Gapdh	TTCACCACCATGGAGAAGGC	CCCTTTTGGCTCCACCCT
Gh	TGAGAAACTGAAGGACCTGGA	GGTTTGCTTGAGGATCTGCC
Igf1	TGGATGCTCTTCAGTTCGTG	GCAACACTCATCCACAATGC
Lhb	AGTCTGCATCACCTTCACCA	TAGGTGCACACTGGCTGAG
Pgk1	TACCTGCTGGCTGCTGGATGG	CACAGCCTCGGCATTATTTCT
Phf6	ACCACTGTGCATTGCATGAT	TGCAGTTTTCTTGTGTTTTCG
Pomc	CATAGATGTGTGGAGCTGGTG	GAGAGGTCGAGTTTGCAAGC
Prl	AGCCCCCGAATACATCCTAT	ATCCCATTTCCTTTGGCTTC
Sst	CCCAGACTCCGTCAGTTTCT	GGGCATCATTCTCTGTCTGG
Trh	CTACCCAGCCAGTTTGCACT	ATCAAAGCCAGAGCCATCAT
Tshb	TGGGTCATCACAGCAGTAACT	GGGAATACAAAAGGATGCTGCT

Table S5: *Phf6$^{-/Y}$* survive on the FVB/BALB/c background

Survival of offspring derived from crossing *Phf6$^{+/-}$* females to *Phf6$^{+/Y}$* males. *Phf6$^{-/Y}$* mice can survive but are under-represented at weaning (pups discarded at ethical endpoint due to low body weight and failure to thrive). Data at each age point were analysed by a Chi-squared test.

	Female		Male		Total	P-value
	Phf6$^{+/+}$	*Phf6$^{+/-}$*	*Phf6$^{+/Y}$*	*Phf6$^{-/Y}$*		
Birth	71 (27.4%)	67 (25.9%)	72 (27.8%)	49 (18.9%)	259	0.15 (3 DF)
Weaning	58 (27.8%)	50 (23.9%)	64 (30.6%)	37 (17.7%)	58	0.0498 (3 DF)

Table S6: PRL secretion parameters

Analysis of data presented in Figure S2. Secretion parameters were calculated using *AutoDecon.* P-value was determined using two-tailed paired T-test for each parameter.

	PRL						
Experimental group	Pair 1		Pair 2		Pair 3		
Genotype	*Phf6$^{+/Y}$*	*Phf6$^{-/Y}$*	*Phf6$^{+/Y}$*	*Phf6$^{-/Y}$*	*Phf6$^{+/Y}$*	*Phf6$^{-/Y}$*	*P-value*
Basal secretion rate (pg/mL per min)	1.14×10^4	7.73×10^4	1.39×10^4	2.16×10^2	10.499	2.0549	0.45
Area under curve	1.18×10^5	79402	1.53E+05	1.63×10^5	95312	86662	0.40
Average concentration (pg/mL)	328.76	220.56	425.66	452.81	264.76	240.73	0.40
Number peaks	1	3	3	1	1	3	0.67
Sum peak mass	289.6	553.16	7895.5	1489.1	783.16	576.07	0.58
Maximum peak mass	289.6	255.02	4736.4	1489.1	783.16	217.96	0.14
Average peak mass	289.6	184.39	2631.83	1489.1	783.16	192.02	0.11

Table S7: TSH secretion parameters

Analysis of data presented in Figure S2. Secretion parameters were calculated using *AutoDecon.* P-value was determined using two-tailed paired T-test for each parameter.

	TSH						
Experimental group	*Pair 1*		*Pair 2*		*Pair 3*		
Genotype	*Phf6$^{+/Y}$*	*Phf6$^{-/Y}$*	*Phf6$^{+/Y}$*	*Phf6$^{-/Y}$*	*Phf6$^{+/Y}$*	*Phf6$^{-/Y}$*	*P-value*
Basal secretion rate (pg/mL per min)	1.49×10^4	17.592	12.87	21.65	9.31×10^5	4.49	0.17
Area under curve	65062	47874	28985	42460	20440	21639	0.85
Average concentration (pg/mL)	180.73	132.98	80.514	117.94	56.78	60.11	0.85
Number peaks	7	4	1	2	7	11	0.66
Sum peak mass	10369.5	5430.66	2245.4	7007.5	343.87	7100.96	0.38
Maximum peak mass	1941.8	1937.4	2245.4	4460.7	106.73	1084.4	0.28
Average peak mass	1481.36	1357.67	2245.4	3503.75	56.00	645.54	0.35

Table S8: ACTH secretion parameters

Analysis of data presented in Figure S2. Secretion parameters were calculated using *AutoDecon.* P-value was determined using two-tailed paired T-test for each parameter.

	ACTH						
Experimental group	*Pair 1*		*Pair 2*		*Pair 3*		
Genotype	*Phf6$^{+/Y}$*	*Phf6$^{-/Y}$*	*Phf6$^{+/Y}$*	*Phf6$^{-/Y}$*	*Phf6$^{+/Y}$*	*Phf6$^{-/Y}$*	*P-value*
Basal secretion rate (pg/mL per min)	1.55×10^4	0.42	5.77	26.48	2.043	9.89	0.23
Area under curve	5235	4775.9	6603.7	10863	5865.7	5545.3	0.60
Average concentration (pg/mL)	14.542	13.266	18.344	30.174	16.294	15.403	0.60
Number peaks	1	2	11	1	1	4	0.94
Sum peak mass	6.10	13.210	3492.57	6066.8	42.90	4227.81	0.27
Maximum peak mass	6.10	7.02	675.06	6066.8	42.90	796.77	0.17
Average peak mass	6.10	6.6049	317.51	6066.8	42.90	1056.95	0.17

Table S9: LH secretion parameters
Analysis of data presented in Figure S2. Secretion parameters were calculated using *AutoDecon.* P-value was determined using two-tailed paired T-test for each parameter.

	LH						
Experimental group	Pair 1		Pair 2		Pair 3		
Genotype	*Phf6[+/Y]*	*Phf6[−/Y]*	*Phf6[+/Y]*	*Phf6[−/Y]*	*Phf6[+/Y]*	*Phf6[−/Y]*	*P-value*
Basal secretion rate (pg/mL per min)	8.90×10^5	0.95	12.281	1.53×10^4	7.47×10^5	1.10×10^3	0.97
Area under curve	85891	62072	9856.5	16343	8375.4	10321	0.65
Average concentration (pg/mL)	238.59	172.42	27.38	45.40	23.27	28.67	0.65
Number peaks	8	1	4	8	1	2	0.83
Sum peak mass	2310.49	102.53	26589.9	610.99	12.77	46.45	0.36
Maximum peak mass	421.06	102.53	5833.2	175.43	12.77	26.75	0.37
Average peak mass	288.81	102.53	6647.48	76.37	12.78	23.23	0.39

Table S10: FSH secretion parameters
Analysis of data presented in Figure S2. Secretion parameters were calculated using *AutoDecon.* P-value was determined using two-tailed paired T-test for each parameter.

	FSH						
Experimental group	Pair 1		Pair 2		Pair 3		
Genotype	*Phf6[+/Y]*	*Phf6[−/Y]*	*Phf6[+/Y]*	*Phf6[−/Y]*	*Phf6[+/Y]*	*Phf6[−/Y]*	*P-value*
Basal secretion rate (pg/mL per min)	15.273	320.57	697.25	7.92E-05	27.366	13.752	0.52
Area under curve	7.31×10^5	6.33×10^5	6.56×10^5	5.30×10^5	5.82×10^5	8.15×10^5	0.97
Average concentration (pg/mL)	2030.5	1759.3	1822.6	1471.1	1616.9	2263.4	0.97
Number peaks	1	5	1	5	2	1	0.39
Sum peak mass	1486.4	57864.9	15714	5844.79	1593.72	2120.2	0.55
Maximum peak mass	1486.4	19082	15714	1525	925.04	2120.2	0.83
Average peak mass	1486.4	11572.98	15714	1168.958	796.86	2120.2	0.93

Table S11: p-values for multiple comparisons between animals with the indicated *Phf6* and *Socs2* genotypes, corresponding to body weight data presented in Figure 5A. Data were analysed by a two-way ANOVA followed by Bonferroni's post-hoc test.

Bonferroni's multiple comparisons test	Mean Diff.	95.00% CI of diff.	Summary	Adjusted P Value
Week 1				
$Phf6^{+/Y};Socs2^{+/+}$ vs. $Phf6^{+/Y};Socs2^{-/-}$	-0.3439	-4.621 to 3.933	ns	>0.99
$Phf6^{+/Y};Socs2^{+/+}$ vs. $Phf6^{-/Y};Socs2^{+/+}$	2.007	-3.232 to 7.245	ns	>0.99
$Phf6^{+/Y};Socs2^{+/+}$ vs. $Phf6^{-/Y};Socs2^{-/-}$	1.184	-3.199 to 5.567	ns	>0.99
$Phf6^{+/Y};Socs2^{-/-}$ vs. $Phf6^{-/Y};Socs2^{+/+}$	2.351	-2.526 to 7.227	ns	>0.99
$Phf6^{+/Y};Socs2^{-/-}$ vs. $Phf6^{-/Y};Socs2^{-/-}$	1.528	-2.415 to 5.471	ns	>0.99
$Phf6^{-/Y};Socs2^{+/+}$ vs. $Phf6^{-/Y};Socs2^{-/-}$	-0.8225	-5.792 to 4.147	ns	>0.99
Week 2				
$Phf6^{+/Y};Socs2^{+/+}$ vs. $Phf6^{+/Y};Socs2^{-/-}$	-0.006750	-4.633 to 4.620	ns	>0.99
$Phf6^{+/Y};Socs2^{+/+}$ vs. $Phf6^{-/Y};Socs2^{+/+}$	5.622	0.1780 to 11.07	*	0.04
$Phf6^{+/Y};Socs2^{+/+}$ vs. $Phf6^{-/Y};Socs2^{-/-}$	4.251	-0.3758 to 8.877	ns	0.09
$Phf6^{+/Y};Socs2^{-/-}$ vs. $Phf6^{-/Y};Socs2^{+/+}$	5.629	0.6590 to 10.60	*	0.02
$Phf6^{+/Y};Socs2^{-/-}$ vs. $Phf6^{-/Y};Socs2^{-/-}$	4.258	0.1998 to 8.315	*	0.03
$Phf6^{-/Y};Socs2^{+/+}$ vs. $Phf6^{-/Y};Socs2^{-/-}$	-1.371	-6.341 to 3.598	ns	>0.99
Week 3				
$Phf6^{+/Y};Socs2^{+/+}$ vs. $Phf6^{+/Y};Socs2^{-/-}$	-0.2517	-4.529 to 4.026	ns	>0.99
$Phf6^{+/Y};Socs2^{+/+}$ vs. $Phf6^{-/Y};Socs2^{+/+}$	8.108	2.870 to 13.35	***	<0.001
$Phf6^{+/Y};Socs2^{+/+}$ vs. $Phf6^{-/Y};Socs2^{-/-}$	6.133	1.750 to 10.52	**	0.001
$Phf6^{+/Y};Socs2^{-/-}$ vs. $Phf6^{-/Y};Socs2^{+/+}$	8.360	3.483 to 13.24	***	<0.001
$Phf6^{+/Y};Socs2^{-/-}$ vs. $Phf6^{-/Y};Socs2^{-/-}$	6.385	2.442 to 10.33	***	<0.001
$Phf6^{-/Y};Socs2^{+/+}$ vs. $Phf6^{-/Y};Socs2^{-/-}$	-1.975	-6.945 to 2.995	ns	>0.99
Week 4				
$Phf6^{+/Y};Socs2^{+/+}$ vs. $Phf6^{+/Y};Socs2^{-/-}$	-3.441	-7.824 to 0.9420	ns	0.23
$Phf6^{+/Y};Socs2^{+/+}$ vs. $Phf6^{-/Y};Socs2^{+/+}$	11.81	6.573 to 17.05	***	<0.001
$Phf6^{+/Y};Socs2^{+/+}$ vs. $Phf6^{-/Y};Socs2^{-/-}$	7.174	2.791 to 11.56	***	<0.001
$Phf6^{+/Y};Socs2^{-/-}$ vs. $Phf6^{-/Y};Socs2^{+/+}$	15.25	10.28 to 20.22	***	<0.001
$Phf6^{+/Y};Socs2^{-/-}$ vs. $Phf6^{-/Y};Socs2^{-/-}$	10.62	6.557 to 14.67	***	<0.001
$Phf6^{-/Y};Socs2^{+/+}$ vs. $Phf6^{-/Y};Socs2^{-/-}$	-4.637	-9.607 to 0.3322	ns	0.08
Week 5				
$Phf6^{+/Y};Socs2^{+/+}$ vs. $Phf6^{+/Y};Socs2^{-/-}$	-6.427	-10.81 to -2.044	***	<0.001
$Phf6^{+/Y};Socs2^{+/+}$ vs. $Phf6^{-/Y};Socs2^{+/+}$	10.90	5.663 to 16.14	***	<0.001
$Phf6^{+/Y};Socs2^{+/+}$ vs. $Phf6^{-/Y};Socs2^{-/-}$	5.630	1.114 to 10.14	**	0.006
$Phf6^{+/Y};Socs2^{-/-}$ vs. $Phf6^{-/Y};Socs2^{+/+}$	17.33	12.36 to 22.30	***	<0.001
$Phf6^{+/Y};Socs2^{-/-}$ vs. $Phf6^{-/Y};Socs2^{-/-}$	12.06	7.856 to 16.26	***	<0.001
$Phf6^{-/Y};Socs2^{+/+}$ vs. $Phf6^{-/Y};Socs2^{-/-}$	-5.272	-10.36 to -0.1855	*	0.04
Week 6				
$Phf6^{+/Y};Socs2^{+/+}$ vs. $Phf6^{+/Y};Socs2^{-/-}$	-7.761	-12.04 to -3.483	***	<0.001
$Phf6^{+/Y};Socs2^{+/+}$ vs. $Phf6^{-/Y};Socs2^{+/+}$	11.29	6.049 to 16.53	***	<0.001
$Phf6^{+/Y};Socs2^{+/+}$ vs. $Phf6^{-/Y};Socs2^{-/-}$	5.419	1.036 to 9.802	**	0.007
$Phf6^{+/Y};Socs2^{-/-}$ vs. $Phf6^{-/Y};Socs2^{+/+}$	19.05	14.17 to 23.92	***	<0.001
$Phf6^{+/Y};Socs2^{-/-}$ vs. $Phf6^{-/Y};Socs2^{-/-}$	13.18	9.236 to 17.12	***	<0.001
$Phf6^{-/Y};Socs2^{+/+}$ vs. $Phf6^{-/Y};Socs2^{-/-}$	-5.869	-10.84 to -0.8989	*	0.01
Week 7				
$Phf6^{+/Y};Socs2^{+/+}$ vs. $Phf6^{+/Y};Socs2^{-/-}$	-8.432	-12.71 to -4.155	***	<0.001
$Phf6^{+/Y};Socs2^{+/+}$ vs. $Phf6^{-/Y};Socs2^{+/+}$	11.90	6.665 to 17.14	***	<0.001
$Phf6^{+/Y};Socs2^{+/+}$ vs. $Phf6^{-/Y};Socs2^{-/-}$	5.160	0.7767 to 9.542	*	0.01
$Phf6^{+/Y};Socs2^{-/-}$ vs. $Phf6^{-/Y};Socs2^{+/+}$	20.34	15.46 to 25.21	***	<0.001
$Phf6^{+/Y};Socs2^{-/-}$ vs. $Phf6^{-/Y};Socs2^{-/-}$	13.59	9.648 to 17.54	***	<0.001
$Phf6^{-/Y};Socs2^{+/+}$ vs. $Phf6^{-/Y};Socs2^{-/-}$	-6.744	-11.71 to -1.774	**	0.002
Week 8				
$Phf6^{+/Y};Socs2^{+/+}$ vs. $Phf6^{+/Y};Socs2^{-/-}$	-9.095	-13.37 to -4.818	***	<0.001
$Phf6^{+/Y};Socs2^{+/+}$ vs. $Phf6^{-/Y};Socs2^{+/+}$	10.61	3.984 to 17.24	***	<0.001
$Phf6^{+/Y};Socs2^{+/+}$ vs. $Phf6^{-/Y};Socs2^{-/-}$	3.356	-1.159 to 7.871	ns	0.29
$Phf6^{+/Y};Socs2^{-/-}$ vs. $Phf6^{-/Y};Socs2^{+/+}$	19.71	13.36 to 26.05	***	<0.001
$Phf6^{+/Y};Socs2^{-/-}$ vs. $Phf6^{-/Y};Socs2^{-/-}$	12.45	8.362 to 16.54	***	<0.001
$Phf6^{-/Y};Socs2^{+/+}$ vs. $Phf6^{-/Y};Socs2^{-/-}$	-7.254	-13.76 to -0.7467	*	0.02

Bonferroni's multiple comparisons test	Mean Diff.	95.00% CI of diff.	Summary	Adjusted P Value
Week 9				
$Phf6^{+/Y};Socs2^{+/+}$ vs. $Phf6^{+/Y};Socs2^{-/-}$	-9.952	-14.23 to -5.674	***	<0.001
$Phf6^{+/Y};Socs2^{+/+}$ vs. $Phf6^{-/Y};Socs2^{+/+}$	10.69	5.454 to 15.93	***	<0.001
$Phf6^{+/Y};Socs2^{+/+}$ vs. $Phf6^{-/Y};Socs2^{-/-}$	3.235	-1.148 to 7.618	ns	0.30
$Phf6^{+/Y};Socs2^{-/-}$ vs. $Phf6^{-/Y};Socs2^{+/+}$	20.64	15.77 to 25.52	***	<0.001
$Phf6^{+/Y};Socs2^{-/-}$ vs. $Phf6^{-/Y};Socs2^{-/-}$	13.19	9.243 to 17.13	***	<0.001
$Phf6^{-/Y};Socs2^{+/+}$ vs. $Phf6^{-/Y};Socs2^{-/-}$	-7.457	-12.43 to -2.488	***	<0.001
Week 10				
$Phf6^{+/Y};Socs2^{+/+}$ vs. $Phf6^{+/Y};Socs2^{-/-}$	-9.487	-14.36 to -4.610	***	<0.001
$Phf6^{+/Y};Socs2^{+/+}$ vs. $Phf6^{-/Y};Socs2^{+/+}$	12.41	6.666 to 18.14	***	<0.001
$Phf6^{+/Y};Socs2^{+/+}$ vs. $Phf6^{-/Y};Socs2^{-/-}$	4.338	-0.6322 to 9.307	ns	0.13
$Phf6^{+/Y};Socs2^{-/-}$ vs. $Phf6^{-/Y};Socs2^{+/+}$	21.89	17.02 to 26.77	***	<0.001
$Phf6^{+/Y};Socs2^{-/-}$ vs. $Phf6^{-/Y};Socs2^{-/-}$	13.82	9.881 to 17.77	***	<0.001
$Phf6^{-/Y};Socs2^{+/+}$ vs. $Phf6^{-/Y};Socs2^{-/-}$	-8.067	-13.04 to -3.098	***	<0.001
Week 11				
$Phf6^{+/Y};Socs2^{+/+}$ vs. $Phf6^{+/Y};Socs2^{-/-}$	-10.90	-15.43 to -6.374	***	<0.001
$Phf6^{+/Y};Socs2^{+/+}$ vs. $Phf6^{-/Y};Socs2^{+/+}$	11.92	6.474 to 17.36	***	<0.001
$Phf6^{+/Y};Socs2^{+/+}$ vs. $Phf6^{-/Y};Socs2^{-/-}$	3.614	-1.013 to 8.240	ns	0.23
$Phf6^{+/Y};Socs2^{-/-}$ vs. $Phf6^{-/Y};Socs2^{+/+}$	22.82	17.94 to 27.70	***	<0.001
$Phf6^{+/Y};Socs2^{-/-}$ vs. $Phf6^{-/Y};Socs2^{-/-}$	14.51	10.57 to 18.46	***	<0.001
$Phf6^{-/Y};Socs2^{+/+}$ vs. $Phf6^{-/Y};Socs2^{-/-}$	-8.305	-13.27 to -3.335	***	<0.001

References

Ardinger, H. H., Hanson, J. W. and Zellweger, H. U. (1984). Borjeson-Forssman-Lehmann syndrome: further delineation in five cases. *Am J Med Genet* **19**, 653-664.

Baumstark, A., Lower, K. M., Sinkus, A., Andriuskeviciute, I., Jurkeniene, L., Gecz, J. and Just, W. (2003). Novel PHF6 mutation p.D333del causes Borjeson-Forssman-Lehmann syndrome. *J Med Genet* **40**, e50.

Birrell, G., Lampe, A., Richmond, S., Bruce, S. N., Gecz, J., Lower, K., Wright, M. and Cheetham, T. D. (2003). Borjeson-Forssman-Lehmann syndrome and multiple pituitary hormone deficiency. *J Pediatr Endocrinol Metab* **16**, 1295-1300.

Carter, M. T., Picketts, D. J., Hunter, A. G. and Graham, G. E. (2009). Further Clinical Delineation of the Borjeson-Forssman-Lehmann Syndrome in Patients with PHF6 Mutations. *Am J Med Genet* **149A**, 246-250.

Crawford, J., Lower, K. M., Hennekam, R. C. M., Van Esch, H., Megarbane, A., Lynch, S. A., Turner, G. and Gecz, J. (2006). Mutation screening in Borjeson-Forssman-Lehmann syndrome: identification of a novel de novo PHF6 mutation in a female patient. *J Med Genet* **43**, 238-243.

de Winter, C. F., van Dijk, F., Stolker, J. J. and Hennekam, R. C. (2009). Behavioural phenotype in Borjeson-Forssman-Lehmann syndrome. *J Intellect Disabil Res* **53**, 319-328.

Declercq, J., Brouwers, B., Pruniau, V. P., Stijnen, P., de Faudeur, G., Tuand, K., Meulemans, S., Serneels, L., Schraenen, A., Schuit, F., et al. (2015). Metabolic and Behavioural Phenotypes in Nestin-Cre Mice Are Caused by Hypothalamic Expression of Human Growth Hormone. *PLoS One* **10**, e0135502.

Dereymaeker, A. M., Fryns, J. P., Hoefnagels, M., Heremans, G., Marien, J. and van den Berghe, H. (1986). The Borjeson-Forssman-Lehmann syndrome. A family study. *Clin Genet* **29**, 317-320.

Matsuo, K., Murano, I. and Kajii, T. (1984). Borjeson-Forssman-Lehmann syndrome in a girl. *Jap J Hum Genet* **29**, 121-126.

Petridou, M., Kimiskidis, V., Deligiannis, K. and Kazis, A. (1997). Borjeson-Forssman-Lehmann syndrome: two severely handicapped females in a family. *Clin Neurol Neurosurg* **99**, 148-150.

Preus, M. (1984). Clinical confusion of the Noonan syndrome with the Borjeson-Forssman-Lehmann syndrome. *Journal of mental deficiency research* **28 (Pt 3)**, 235-238.

Robinson, L. K., Jones, K. L., Culler, F., Nyhan, W. L., Sakati, N. and Jones, K. L. (1983). The Borjeson-Forssman-Lehmann syndrome. *Am J Med Genet* **15**, 457-468.

Turner, G., Gedeon, A., Mulley, J., Sutherland, G., Rae, J., Power, K. and Arthur, I. (1989). Borjeson-Forssman-Lehmann syndrome: clinical manifestations and gene localization to Xq26-27. *Am J Med Genet* **34**, 463-469.

Weber, F. T., Frias, J. L., Julius, R. L. and Felman, A. H. (1978). Primary hypogonadism in the Borjeson-Forssman-Lehmann syndrome. *J Med Genet* **15**, 63-66.

Zhang, X., Fan, Y., Liu, X., Ang Zhu, M., Sun, Y., Yan, H., He, Y., Ye, X., Gu, X. and Yu, Y. (2019). A Novel Nonsense Mutation of PHF6 in a Female with Extended Phenotypes of Borjeson-Forssman-Lehmann Syndrome. *J Clin Res Pediatr Endocrinol*.